Technical Report
Research Project T9903, Task 41
Seismic Bridge Restrainers

UNSEATING OF SIMPLY SUPPORTED SPANS DURING EARTHQUAKES

by

Panos Trochalakis
Graduate Research Assistant
Department of Civil Engineering

Marc O. Eberhard
Assistant Professor
Department of Civil Engineering

John F. Stanton
Professor
Department of Civil Engineering

Washington State Transportation Center (TRAC)
University of Washington, Box 354802
University District Building
1107 NE 45th Street, Suite 535
Seattle, Washington 98105-4631

Washington State Department of Transportation
Technical Monitor
Jim Wei
Special Project Engineer

Prepared for

Washington State Transportation Commission
Department of Transportation
and in cooperation with
U.S. Department of Transportation
Federal Highway Administration

May 1996

TECHNICAL REPORT STANDARD TITLE PAGE

1. REPORT NO.	2. GOVERNMENT ACCESSION NO.	3. RECIPIENT'S CATALOG NO.
WA-RD 387.2		

4. TITLE AND SUBTITLE	5. REPORT DATE
UNSEATING OF SIMPLY SUPPORTED SPANS DURING EARTHQUAKES	May 1996
	6. PERFORMING ORGANIZATION CODE
7. AUTHOR(S)	8. PERFORMING ORGANIZATION REPORT NO.
Panos Trochalakis, Marc O. Eberhard, John F. Stanton	
9. PERFORMING ORGANIZATION NAME AND ADDRESS	10. WORK UNIT NO.
Washington State Transportation Center (TRAC) University of Washington, Box 354802 University District Building; 1107 NE 45th Street, Suite 535 Seattle, Washington 98105-4631	11. CONTRACT OR GRANT NO. Agreement T9903, Task 41
12. SPONSORING AGENCY NAME AND ADDRESS	13. TYPE OF REPORT AND PERIOD COVERED
Washington State Department of Transportation Transportation Building, MS 7370 Olympia, Washington 98504-7370	Technical report
	14. SPONSORING AGENCY CODE

15. SUPPLEMENTARY NOTES

This study was conducted in cooperation with the U.S. Department of Transportation, Federal Highway Administration.

16. ABSTRACT

The Washington State Department of Transportation (WSDOT) is currently retrofitting many older bridges to prevent their superstructures from unseating during earthquakes. In bridges whose simply supported spans have inadequate bearing lengths, WSDOT most frequently connects adjacent spans with high-strength rod restrainers. The study described in this report was undertaken to determine whether restrainers installed in this manner are effective in preventing span unseating and to develop a method for identifying vulnerable simply supported spans. A companion report considered the design of seismic restrainers for in-span hinges.

The researchers developed a nonlinear analytical model of a four-span, simply supported, prestressed concrete bridge. Variations of this model were subjected to four ground motions to determine the maximum relative displacements between the simply supported spans and their supports. The maximum relative displacements at the piers depended most on the bearing friction resistance, the earthquake motion, and the size of the joints in the deck. The maximum relative displacements at the abutments depended most on the bearing resistance and the earthquake motion.

Based on the results of the parametric study, the researchers developed a new method to estimate the susceptibility of bridges to unseating of simply supported spans. The researchers also found that restrainers connecting adjacent spans are ineffective in reducing the relative displacements between the superstructure spans and their supports.

17. KEY WORDS	18. DISTRIBUTION STATEMENT
Bridge, design, unseating, span, earthquakes, evaluation	No restrictions. This document is available to the public through the National Technical Information Service, Springfield, VA 22616

19. SECURITY CLASSIF. (of this report)	20. SECURITY CLASSIF. (of this page)	21. NO. OF PAGES	22. PRICE
None	None	45	

DISCLAIMER

The contents of this report reflect the views of the authors, who are responsible for the facts and the accuracy of the data presented herein. The contents do not necessarily reflect the official views or policies of the Washington State Transportation Commission, Department of Transportation, or the Federal Highway Administration. This report does not constitute a standard, specification, or regulation.

TABLE OF CONTENTS

LIST OF FIGURES

LIST OF TABLES

CHAPTER 1

INTRODUCTION

1.1 CONTEXT

The Washington State Department of Transportation (WSDOT) is currently retrofitting superstructures of many existing bridges (Lwin and Henley, 1993) to prevent span unseating during earthquakes. The majority of this retrofit work involves installation of high-strength steel rod restrainers at hinges and joints, and the extension of abutment seats. In designing these retrofit measures, WSDOT currently follows the American Association of State and Highway Transportation Officials (AASHTO) restrainer design guidelines (AASHTO, 1992).

Findings from a study on the use of restrainers at in-span hinges were presented in an earlier report (Trochalakis et al., 1995). This report addresses the application of restrainers in multi-span, simply supported bridges. In these bridges, the spans are structurally separate and each one is simply supported. In such bridges, WSDOT connects adjacent spans with restrainers, but girders are not connected to the pier cap. This study was undertaken to determine whether restrainers installed in this manner are effective and to develop a method for identifying bridges that are susceptible to span unseating.

1.2 OBJECTIVES

The objectives of this study were as follows:

1. to identify the factors that significantly affect the maximum displacement of the superstructure relative to the piers when restrainers are not used

2. to identify the factors that significantly affect the maximum displacement of the superstructure relative to the abutments when restrainers are not used

3. to determine the circumstances, if any, under which restrainers connecting adjacent spans are effective in reducing the maximum displacement of the superstructure relative to the piers

4. to develop a method for identifying simply supported bridges that are prone to span unseating.

1.3 SCOPE OF REPORT

This study was conducted by performing nonlinear time history analyses on a computer model of a bridge. The bridge was selected to represent a freeway overpass with four simply supported spans. The bridge was straight and possessed no skew, and the ground motion was coherent and acted longitudinally. Consideration of other conditions lay outside the scope of this study. Parameters in the model were varied to investigate their influence on response. The development of the standard bridge model and the standard input ground motion are described in Chapter 2. Chapter 3 discusses variations of the standard model and ground motion that were considered in the parametric study. In this study, the bearing pad friction resistance, pier heights, abutment properties, ground motion, and compression gaps were varied. The effectiveness of restrainers connecting adjacent spans is also discussed in this chapter.

Chapter 4 introduces a new method for predicting the unrestrained maximum relative displacement between the superstructure and the bearings (maximum relative bearing displacement, MRBD) of a simply supported bridge. A new procedure for estimating the maximum relative displacement between the abutments and the adjacent

spans (maximum relative abutment displacement, MRAD) is also presented. The proposed method is based on the results of 52 nonlinear time-history analyses. The conclusions and recommendations of this study are presented in Chapter 5.

CHAPTER 2

DEVELOPMENT OF STANDARD BRIDGE MODEL

The model described in this chapter represents a four-span, simply supported, prestressed concrete bridge (Figure 2.1). Only longitudinal motion was taken into account. An analytical model of the bridge was constructed. A standard case was defined in which the parameters in the model were assigned values believed to be representative of those commonly found in practice. In the parametric study described in Chapter 3, the values of some parameters were varied while the others retained their standard values.

2.1 PIER PROPERTIES

Each pier was modeled as a single-degree-of-freedom system, the weight of which represented the weight (W_{cap}=636 KN=143 kips) of the pier cap and one half of the columns (Figure 2.1). A yielding spring represented the stiffness and strength of each supporting pier, acting as a cantilever.

The dead load transferred to each pier was computed on the basis of the span lengths, widths, and cross-sections shown in Figure 2.1. The number and size of the piers were selected assuming the use of standard, 3-ft-diameter columns and an average axial stress under dead load of $0.1f_c'$, where f_c' = 27.6 MPa (4000 psi). Three columns were necessary. Using this axial compressive stress, a longitudinal reinforcement ratio of 1 percent, and grade 60 reinforcement, the cracked section moment of inertia ($I_{cracked}$) of each column was calculated to be 0.0125 m^4 (30,000 in^4), assuming linear material

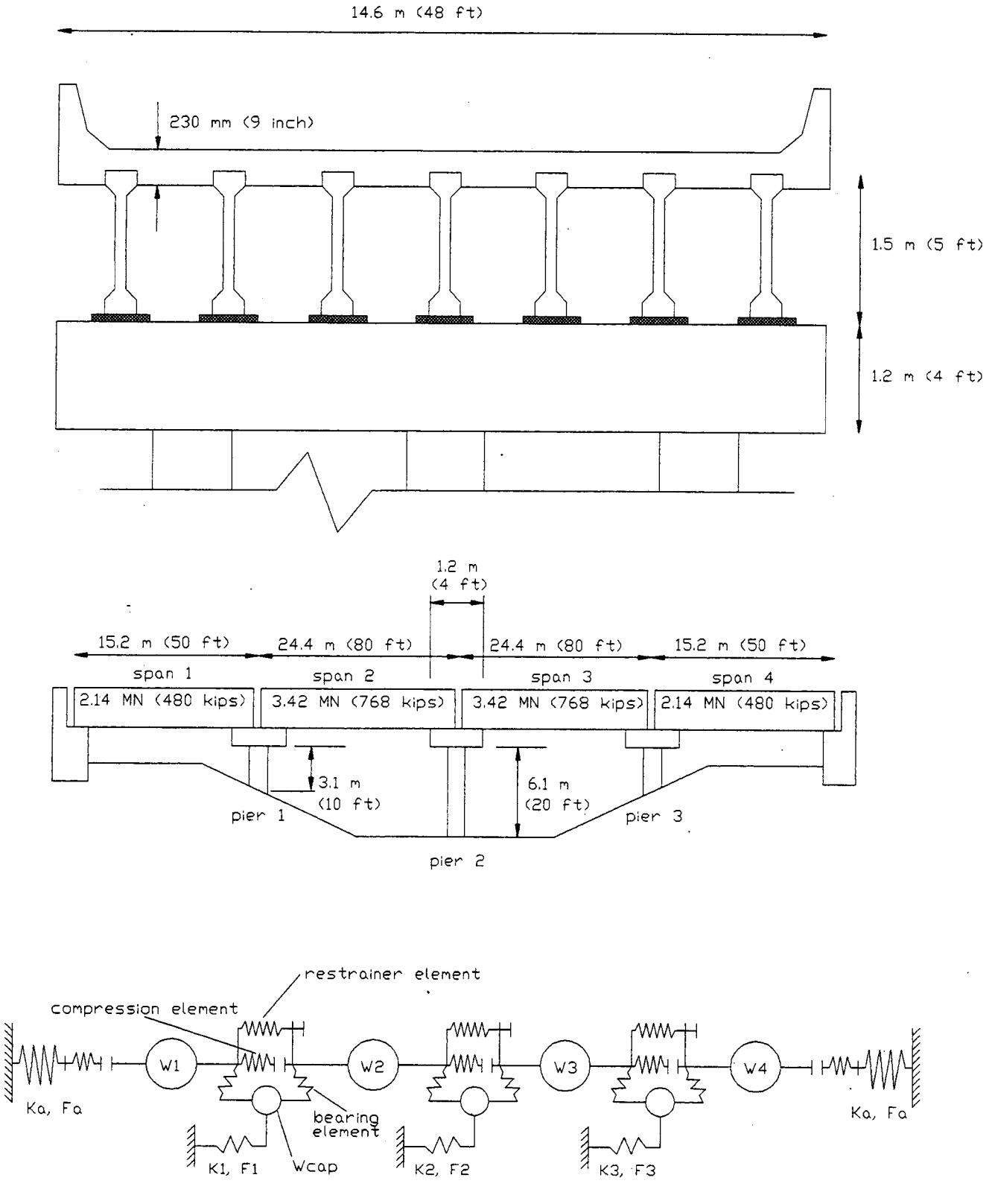

Figure 2.1. Standard Bridge Model

behavior and a cracked section. This value is approximately 35 percent of the gross section moment of inertia. The longitudinal stiffness and strength of each pier were assumed to be those of a cantilever. Therefore, the stiffness of each pier was calculated as follows:

$$K = (\#\text{ of columns}) * 3\, EI_{cracked} / H^3 \qquad (2.1)$$

where

H = height of pier

E = modulus of elasticity of concrete (24.7 Gpa = 3582 ksi)

$I_{cracked}$ = cracked section moment of inertia

These values imply that the footing is rigid. In practice this is not the case, but the effect of footing flexibility was assumed to be small in comparison to the reduction in column stiffness due to cracking. All the columns within a pier were assumed to yield at their base. Therefore, the pier yield force was computed as follows:

$$F = (\#\text{ of columns}) * M_{yield} / H \qquad (2.2)$$

where

M_{yield} = yield moment (1130 KN-mm = 10,000 kip-in.)

M_{yield} was computed assuming linear material behavior, a cracked cross-section, and an axial load of $0.1\, f_c' A_g$. For the standard case, the center pier had a height of 6.1 m (20 ft) and the outside piers had a height of 3.1 m (10 ft). Therefore, the center pier had a stiffness of 12.3 KN/mm (70 kips/in.) and a strength of 560 KN (125 kips). The outside piers had a stiffness of 98.8 KN/mm (562.5 kips/in.) and a strength of 1.1 MN (250 kips). The elements representing the piers had a strain hardening ratio of 2 percent.

2.2 ABUTMENT PROPERTIES

Seat abutments with elastomeric bearing pads but without restrainers were included in the model. The abutment backwall was assumed to shear off at the bottom of the superstructure, so the computed abutment strength and stiffness were based on a soil area with dimensions equal to those of the superstructure (14.6 m wide (48 ft) and 1.5 m deep (5 ft)). The stiffness and strength were calculated using the Caltrans recommended values of 115 KN/mm per linear meter (200 kips/in. per linear foot) and a soil strength of 53.1 Mpa (7.7 kips per square foot of abutment backwall) (California Department of Transportation 1989). Both of these values are based on a 2.44-m (8-ft) deep soil wedge. The stiffness and strength were assumed to vary as the height squared. For a unit width of soil wedge and a constant inclination of the slip plane, the weight of the wedige varies with the square of the depth. In a cohesionless soil, the strength is derived from friction, which therefore also varies with the square of the depth. For consistency, the same assumption was also made for the stiffness. Therefore, the adjusted values for the superstructure depth (1.5 m = 5 ft) resulted in an abutment stiffness of 659 KN/mm (3750 kips/in.) and a strength of 5.08 MN (1155 kips).

2.3 JOINT PROPERTIES

The joint model (Figure 2.2) consisted of three types of elements. A linear spring modeled the impact of two adjacent spans. This spring was effective only in compression and had an initial gap of 25 mm (1 in.). Its stiffness (17.5 MN/mm = 100,000 kips/in.) represented the axial stiffness of the superstructure.

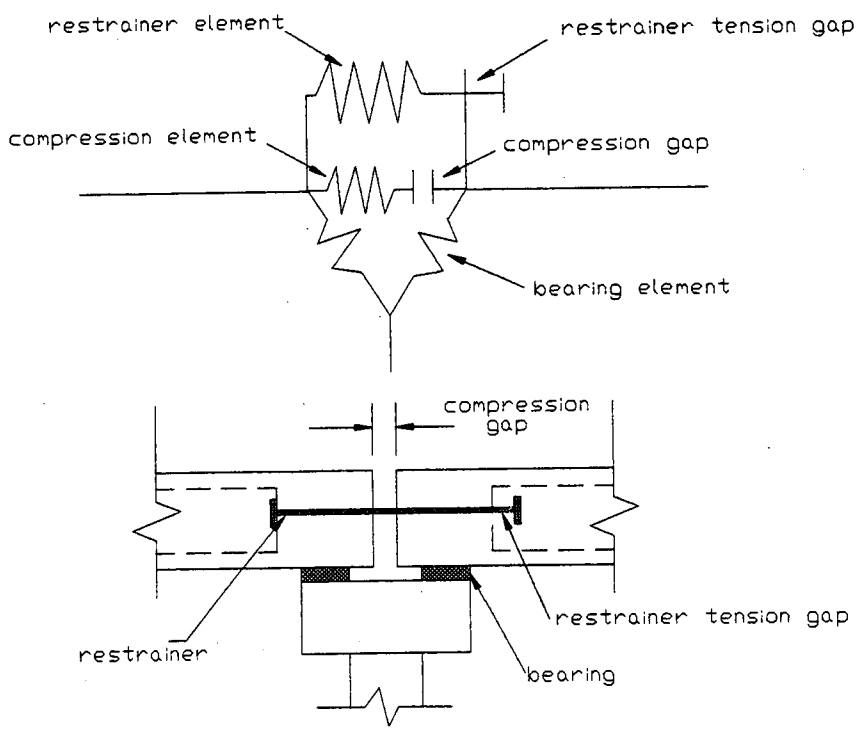

Figure 2.2. Two Span Joint Model

The elastomeric bearing pads were modeled with nonlinear elements that had no gap. The stiffness of the pads was calculated as follows:

$$K_{pads} = (\#\ of\ pads) * GA / t \tag{2.3}$$

where

G = shear modulus of bearing pads

A = area of bearing pads

t = thickness of bearing pads

The number of bearing pads at each pier cap was equal to the number of beams it supported. Seven pads were used to calculate the properties of each bearing element.

Assuming that the bearing pads measured 0.56 m by 0.23 m by 25 mm (22 in. x 9 in. x 1 in.) and had a shear modulus of 1.03 Mpa (150 psi), the stiffness was computed to be 36.8 KN/mm (210 kips/in.). The force on the bearings at which sliding occurs was calculated by assuming a coefficient of friction of 0.30. Using the span weights shown in Figure 2.1, the bearing strengths were computed to be 317 KN (72 kips) for the 15.2-m (50-ft) spans and 507 KN (115 kips) for the 24.3-m (80-ft) spans.

The third type of element was a linear spring that modeled the seismic restrainers. This element had an initial gap of 25 mm and was effective only in tension. The standard case had a value of zero for the restrainer stiffness.

2.4 DAMPING

Viscous damping was assumed to be 5 percent of critical. Because damping was based on the initial stiffness matrix, only elements without an initial gap were used to calculate the mass and stiffness proportional damping.

2.5 COMPUTED RESPONSE

The ground motion used in the standard analysis was the North-South component of the 1940 El Centro earthquake (Figure 2.3). The record was scaled by a factor of 2 to obtain a peak acceleration of 0.70 g.

For the standard case, the maximum MRBD (maximum relative bearing displacement) occurred at the right bearing over pier 1 (Figure 2.1). The responses of pier 1 and span 2 are shown in Figure 2.4. Positive displacement denotes displacement to the right in Figure 2.1. Only span displacements away from the pier could result in span

unseating. Therefore, the MRBD calculation considered only the displacements of the superstructure away from the pier cap. For the standard case, the maximum MRBD was 91 mm (3.6 in.) and occurred 5.36 seconds into the ground motion.

The largest MRAD occurred at the right abutment. Because the abutment backwall was modeled as shearing off during the earthquake, the abutment seat was assumed to remain in its initial position. Therefore, the definition of MRAD included only span displacements away from the initial abutment position. That is, the MRAD at abutment 2 was the maximum negative span displacement. This definition may be slightly unconservative because the abutment seat would be expected to move some amount during the earthquake. The displacement response of span 4 is shown in Figure 2.5. The MRAD of 85 mm (3.4 in.) occurred at a time of 2.36 sec.

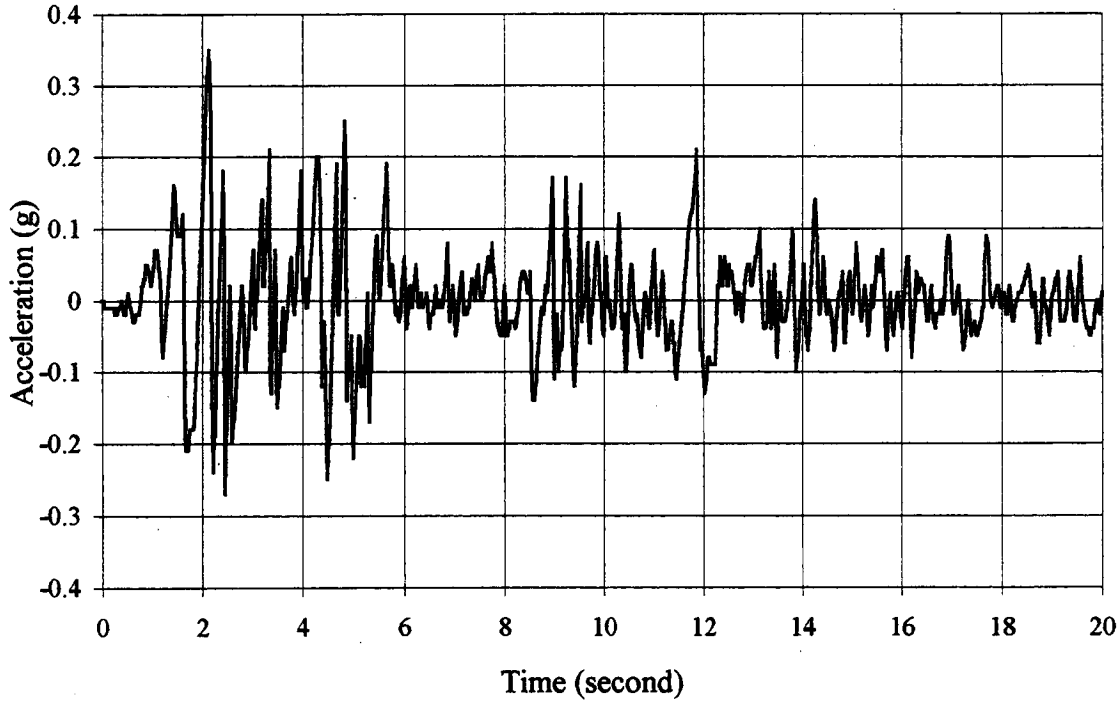

Figure 2.3. N-S Component of 1940 El Centro Earthquake

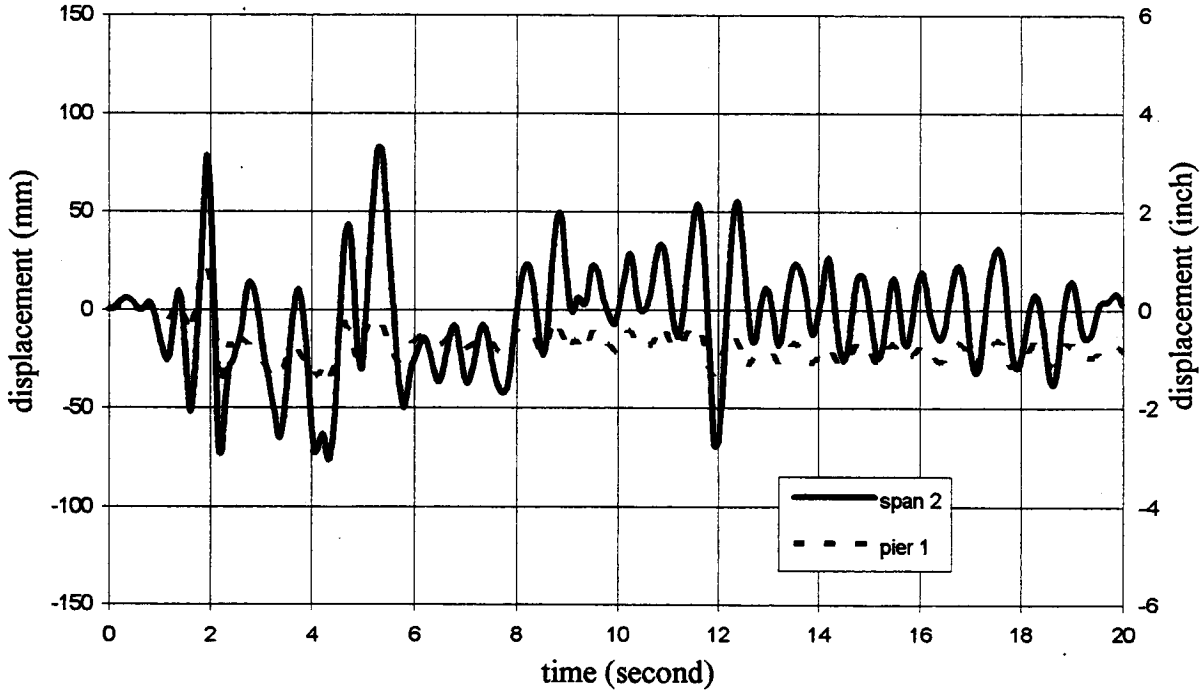

Figure 2.4. Response of Pier 1 and Span 2

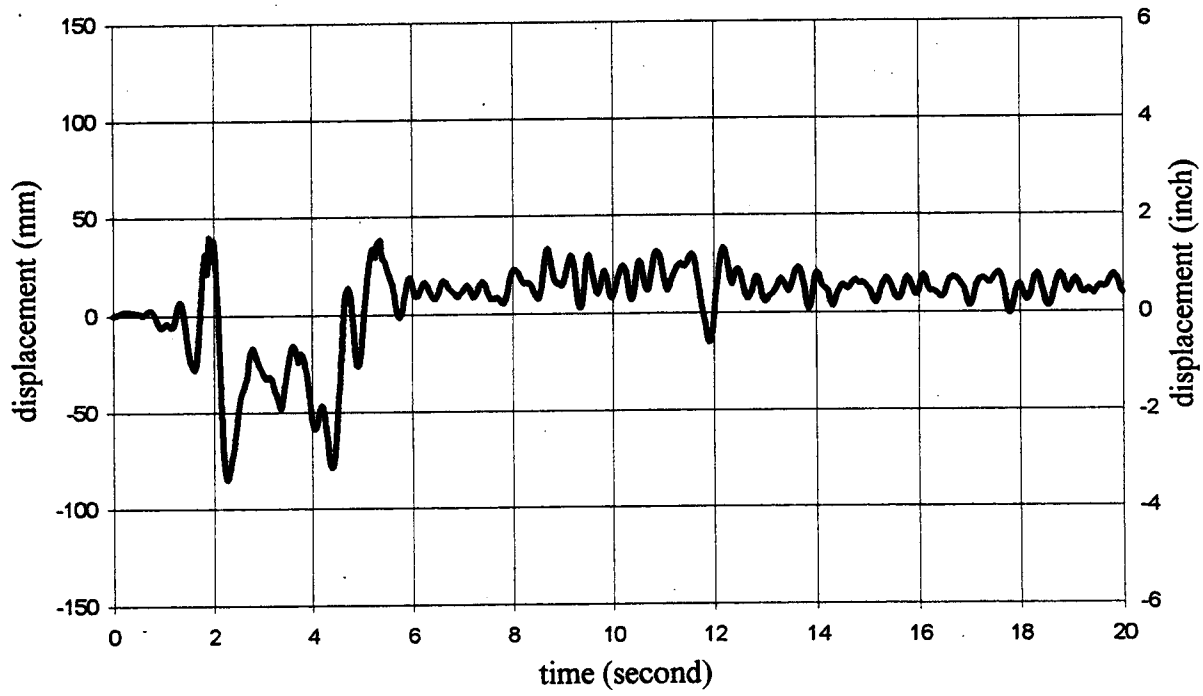

Figure 2.5. Response of Span 4

CHAPTER 3

PARAMETRIC STUDY

A parametric study was conducted on the unrestrained model to identify the factors important in predicting span unseating. This chapter summarizes the parameters varied, their ranges, and the results of the variation. The results of the parametric study were used to develop a method for identifying bridges that are prone to span unseating. Further analyses were conducted to evaluate the effectiveness of restrainers connecting adjacent spans.

3.1 OVERVIEW OF STUDY

The five parameters varied, along with their respective ranges, are listed in Table 3.1.

Table 3.1. Parameters and Ranges

Parameter	Range
Pier Heights	3.1 m (10 ft) to 9.1 m (30 ft)
Abutment Factor (stiffness and strength)	1/4 to 1
Earthquake Record and Intensity	El Centro*2, James Rd*1, Pacoima*1, Olympia*2
Compression Gap	25 mm (1 in.) to 50 mm (2 in.)
Bearing Factor (stiffness and friction)	1/8 to 1
Restrainer Stiffness	0 or 88 KN/mm (0 or 500 K/in.)

Each parameter was varied independently while the remaining properties were kept constant. For each case, the bearing friction force was varied from 1/8 times the standard value to the full value of the standard bearing friction force.

Two plots are shown for each parameter varied. The first plot shows the effect of the parameter on the maximum MRBD, and the second shows the effect on the maximum MRAD. For all the plots, the x-axis consists of the bearing factor, which is defined as the ratio of the bearing resistance used in the analysis to the standard bearing resistance (see Section 2.3).

3.2 EFFECT OF BEARING PAD FRICTION

The effect of bearing pad friction on the response of the standard model is evident in Figure 3.1. A decrease in the bearing pad friction resulted in increased MRBDs and MRADs.

3.3 EFFECT OF PIER HEIGHT

Four bridge configurations were studied to investigate the effect of pier height on the MRBD and MRAD. The four configurations are described in Table 3.2. As shown in Figure 3.2, the effect of pier height on the MRBD showed no clear trend. In a few cases, changing the height of the piers resulted in a large change in the MRBD. In other cases, the change was insignificant. The effect of pier height on the MRAD was minor (Figure 3.2), typically less than 25 mm (1 in.).

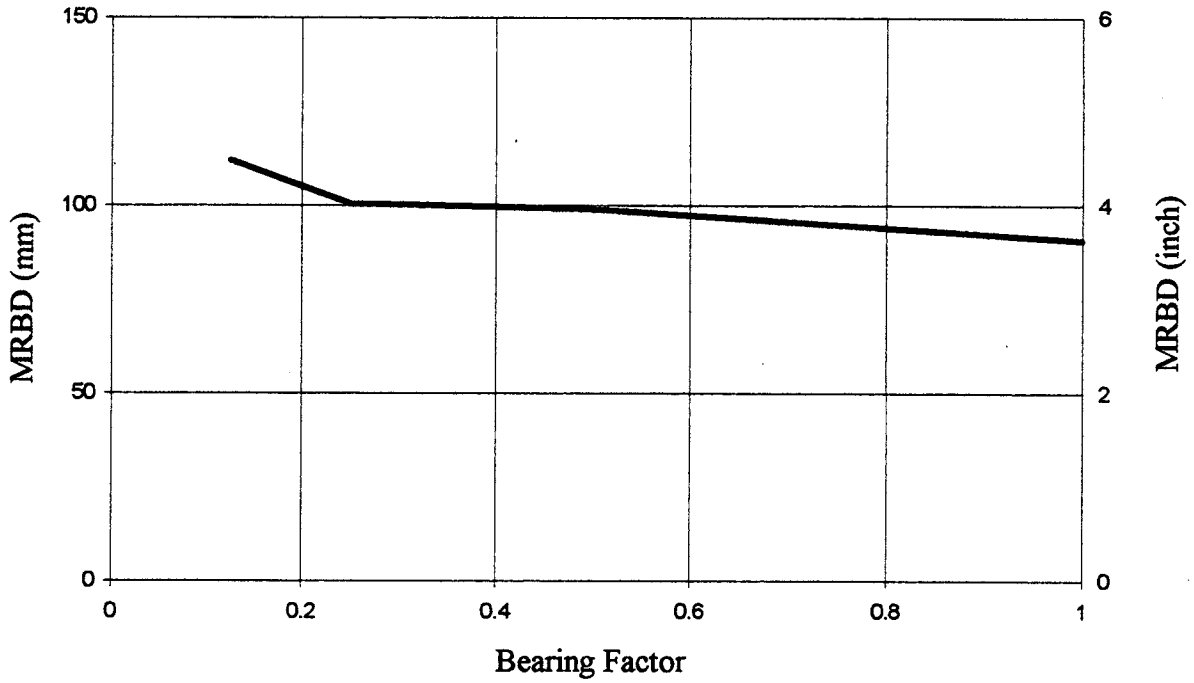

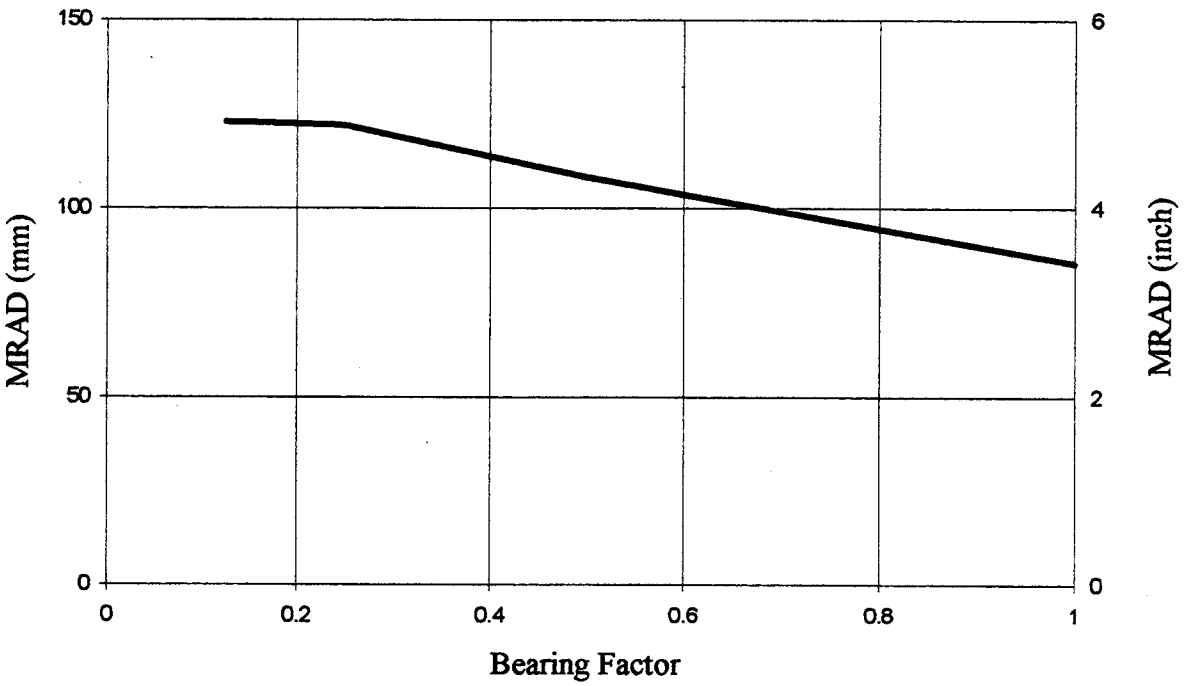

Figure 3.1. Effect of Bearing Strength

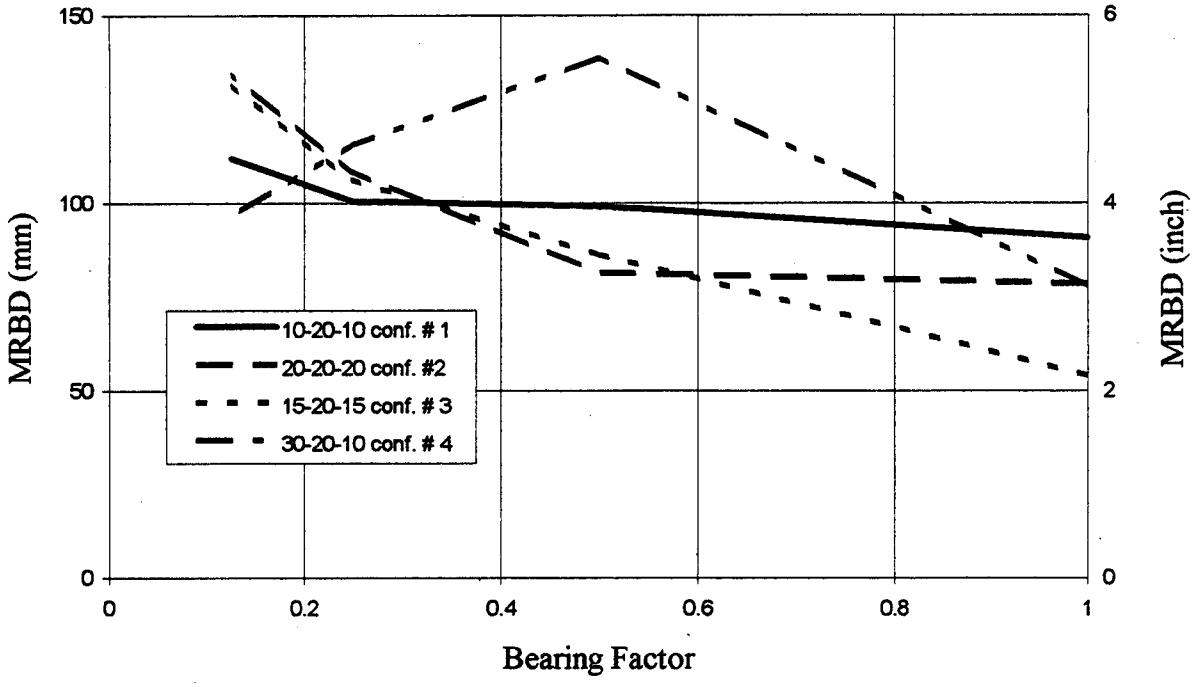

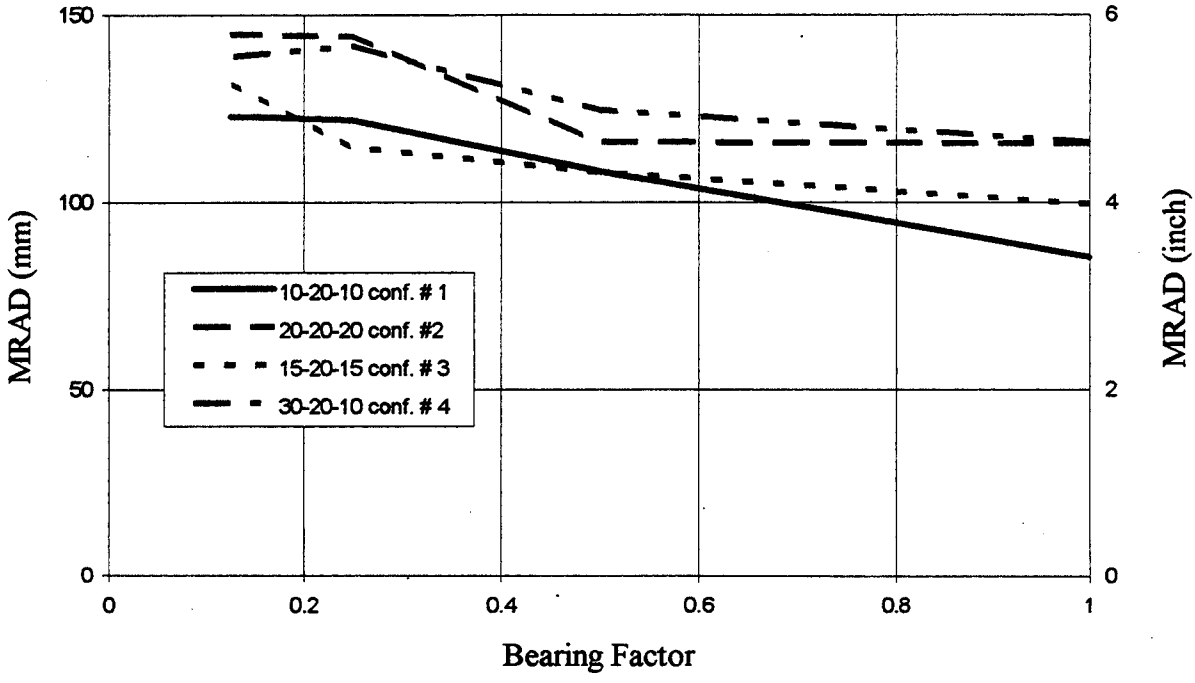

Figure 3.2. Effect of Pier Height

Table 3.2. Configurations for Pier Height Parameter

Configuration #	Pier 1 Height	Pier 2 Height	Pier 3 Height
1	3.1 m (10 ft)	6.1 m (20 ft)	3.1 m (10 ft)
2	6.1 m (20 ft)	6.1 m (20 ft)	6.1 m (20 ft)
3	4.6 m (15 ft)	6.1 m (20 ft)	4.6 m (15 ft)
4	9.1 m (30 ft)	6.1 m (20 ft)	3.1 m (10 ft)

3.4 EFFECT OF ABUTMENT FACTOR

Multiplying the abutment stiffness and strength by factors of 0.25 and 0.5 resulted in minor changes in the maximum MRBD and the maximum MRAD (Figure 3.3). A decrease in the abutment resistance generally increased the MRBD by about 25 mm (1 in.).

3.5 EFFECT OF EARTHQUAKE RECORD AND INTENSITY

The earthquake record and intensity used in the analysis significantly affected the maximum MRBD and MRAD (Figure 3.4). For the majority of the cases, the earthquake motion with the largest peak ground acceleration produced the largest relative displacement.

3.6 EFFECT OF COMPRESSION GAP

Changing the compression gap from 25 mm (1 in.) to 50 mm (2 in.) resulted in an additional 25 to 50 mm (1 to 2 in.) in the maximum MRBD (Figure 3.5). The MRAD was affected by variations in the compression gap, but the results showed no clear trend.

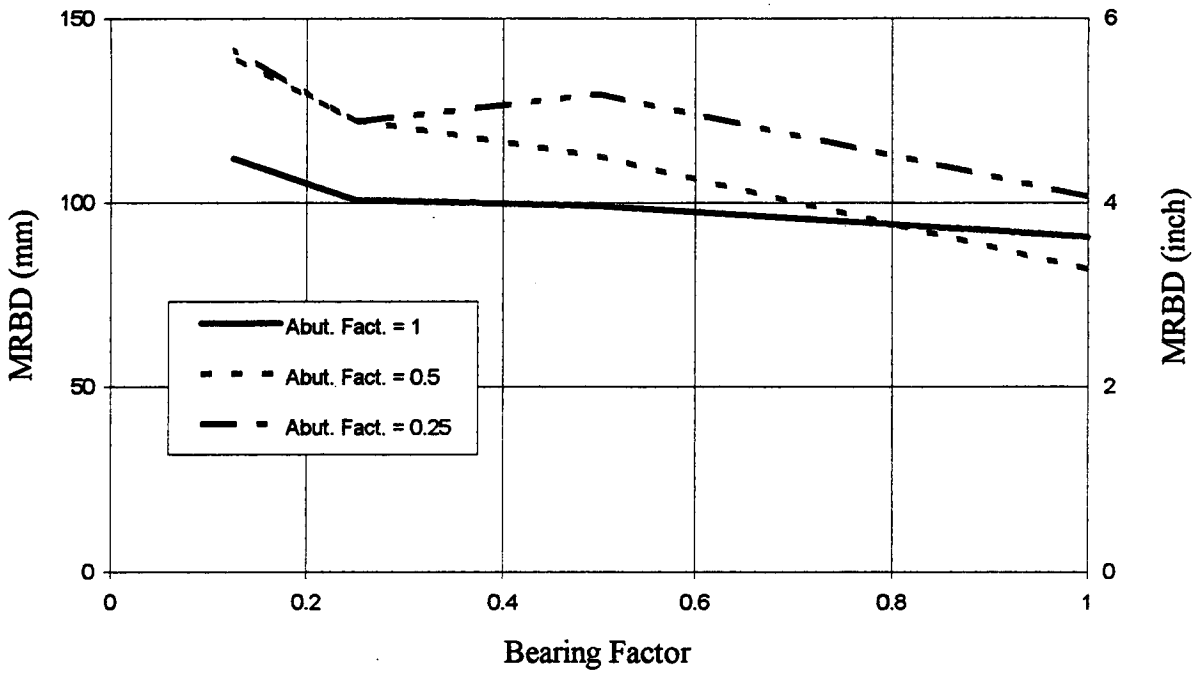

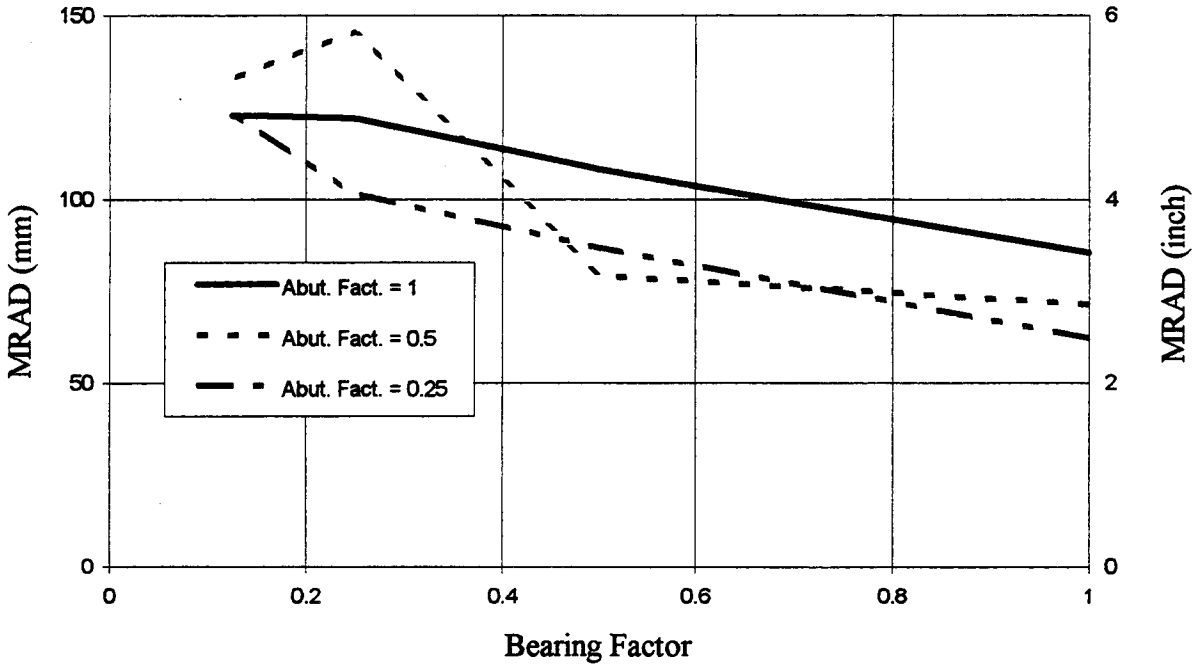

Figure 3.3. Effect of Abutment Factor

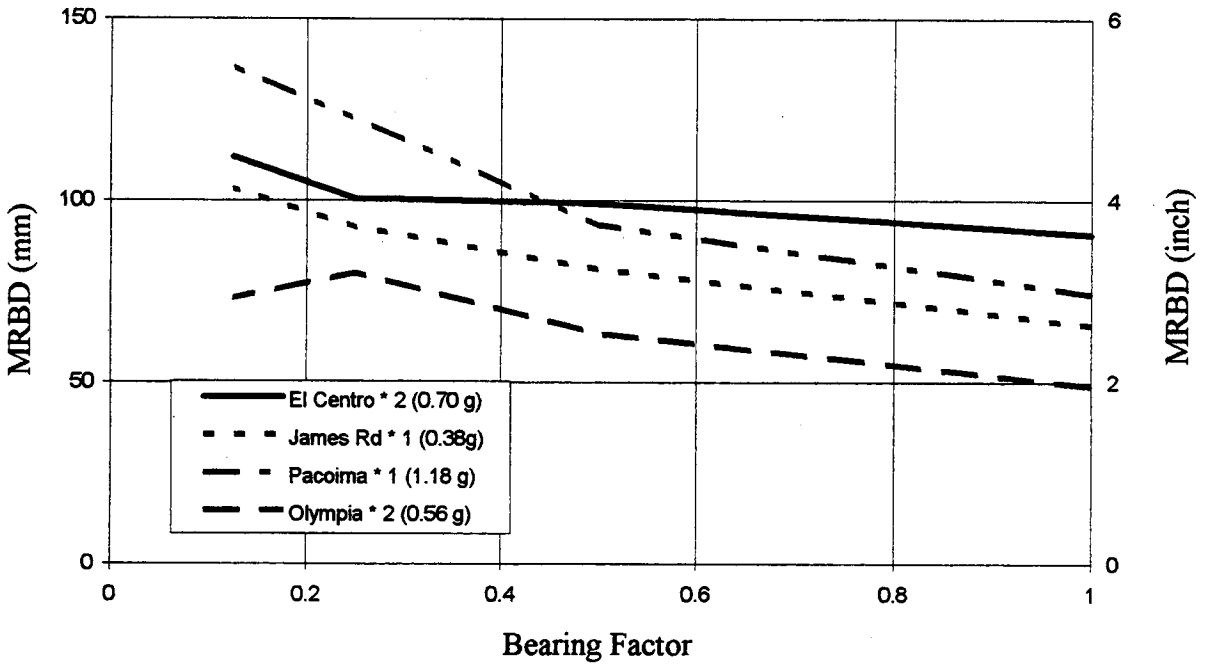

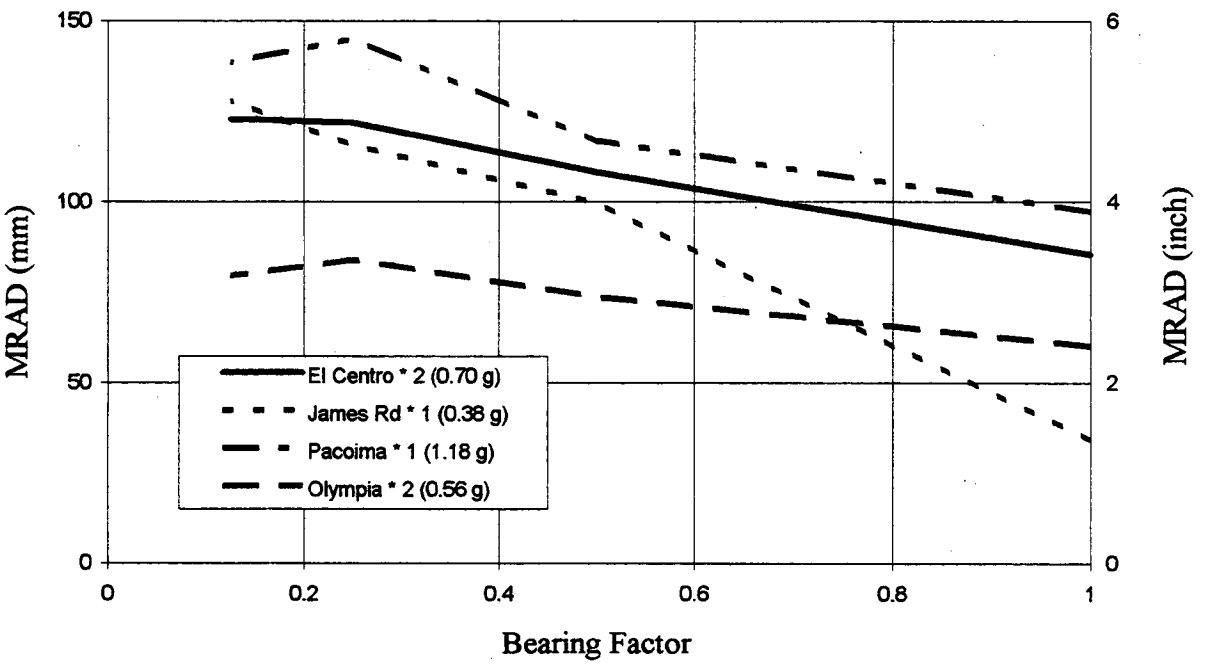

Figure 3.4. Effect of Earthquake Record and Intensity

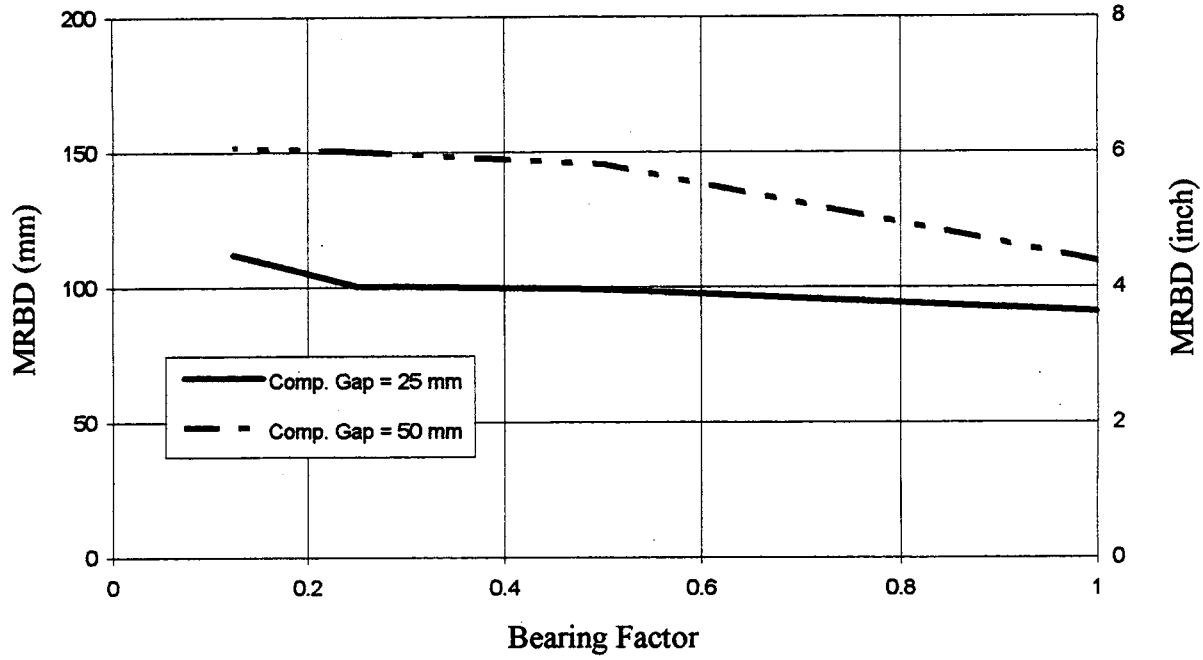

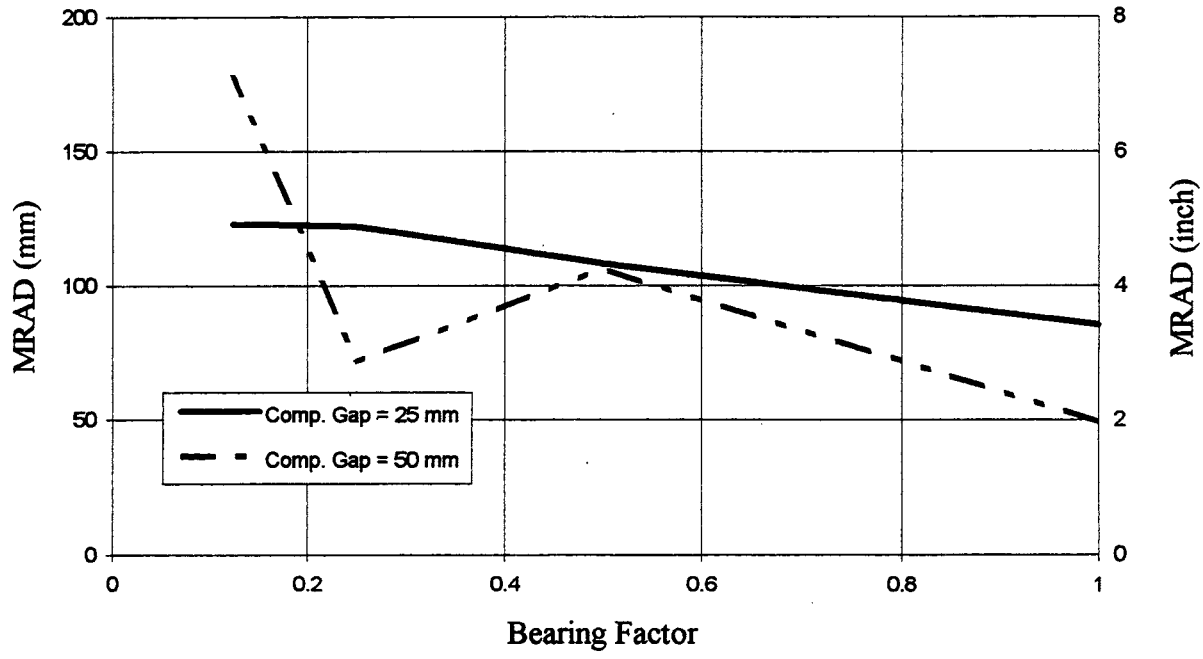

Figure 3.5. Effect of Compression Gap

3.7 EFFECT OF RESTRAINERS CONNECTING ADJACENT SPANS

Figures 3.6 through 3.9 show a comparison between the restrained and unrestrained responses of the four models described in Table 3.2. For all four models, the restrained and unrestrained cases were analyzed through the range consisting of 1/8 to 1 times the standard bearing friction strength. Each figure includes three plots. The first plot compares the maximum MRBD of the restrained case with that of the unrestrained case. The second plot shows the effect of restrainers on the MRAD. The third plot shows how the restrainers affected the maximum relative displacement between adjacent spans (MRDBS). If this relative displacement exceeded the restrainer gap, the restrainers were activated. For all restrained cases, the restrainer stiffness was 87.6 KN/mm (500 kips/in.) and the restrainer tension gap was 25 mm (1 in.).

In all the restrained cases, the restrainers were activated. The restrainers were ineffective in reducing the MRBD. However, for all cases except one (configuration #4), restrainers connecting adjacent spans did not significantly affect the maximum MRBD or MRAD.

3.8 DISCUSSION

The largest MRBD and MRAD were both less than 150 mm (6 in.) for all parameter values except a compression gap of 50 mm (2 in.). This relative displacement is small enough that it would not lead to unseating in many bridges. Even in the rather extreme combination of a bearing factor equal to 1/8 and a compression gap of 50 mm (2 in.), the MRBD was approximately 150 mm (6 in.) and the MRAD was approximately 175 mm (7 in.).

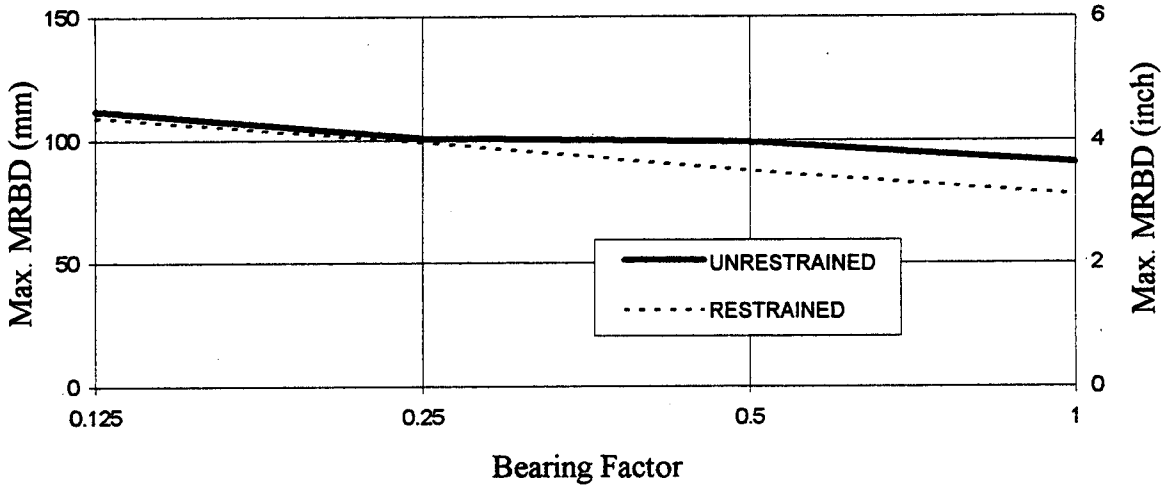

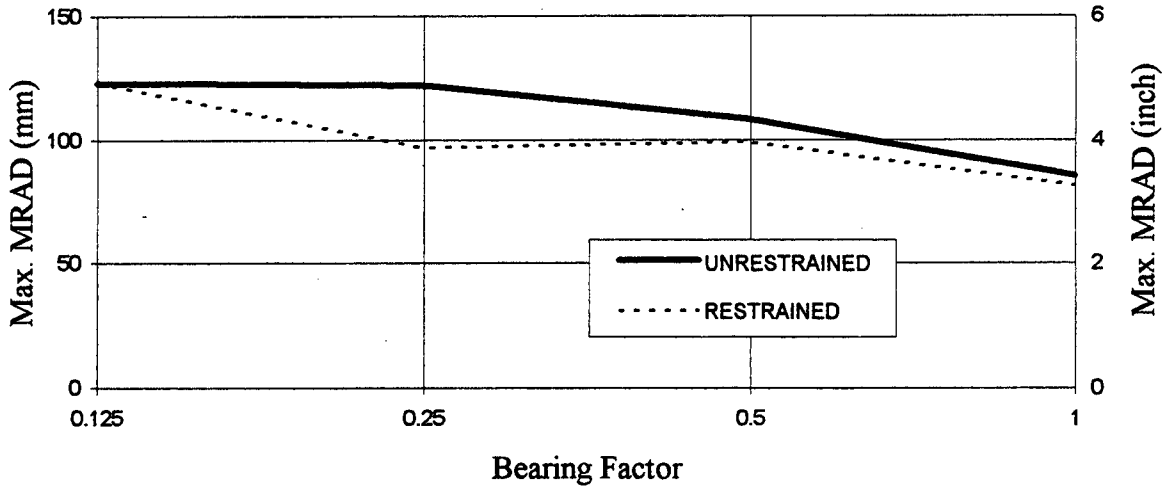

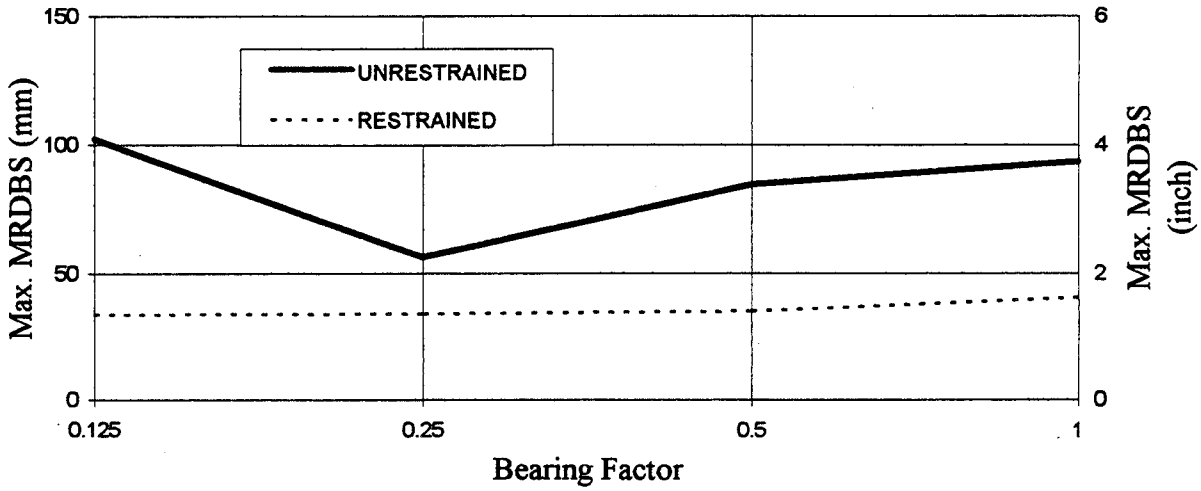

Figure 3.6. Effect of Restrainers on Configuration # 1

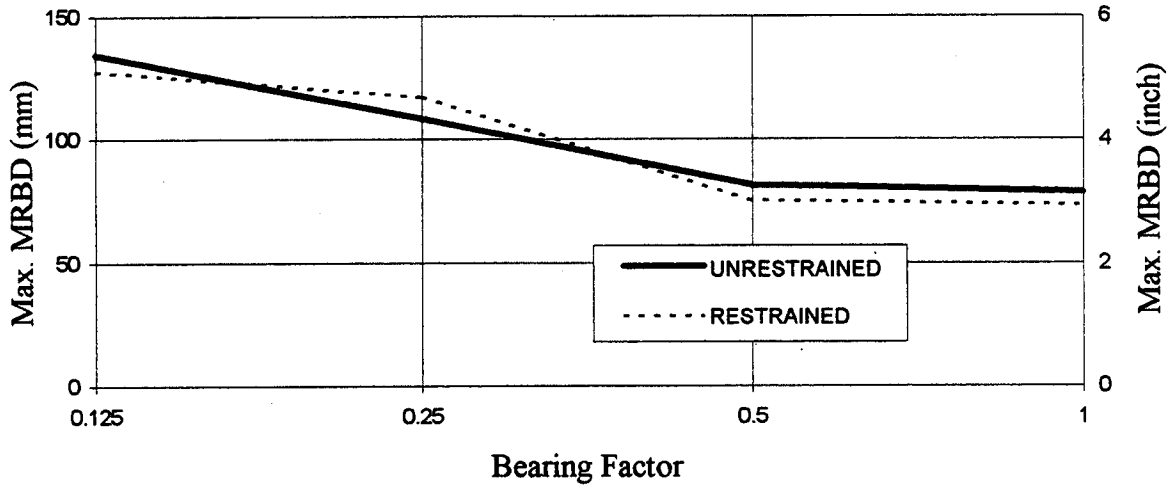

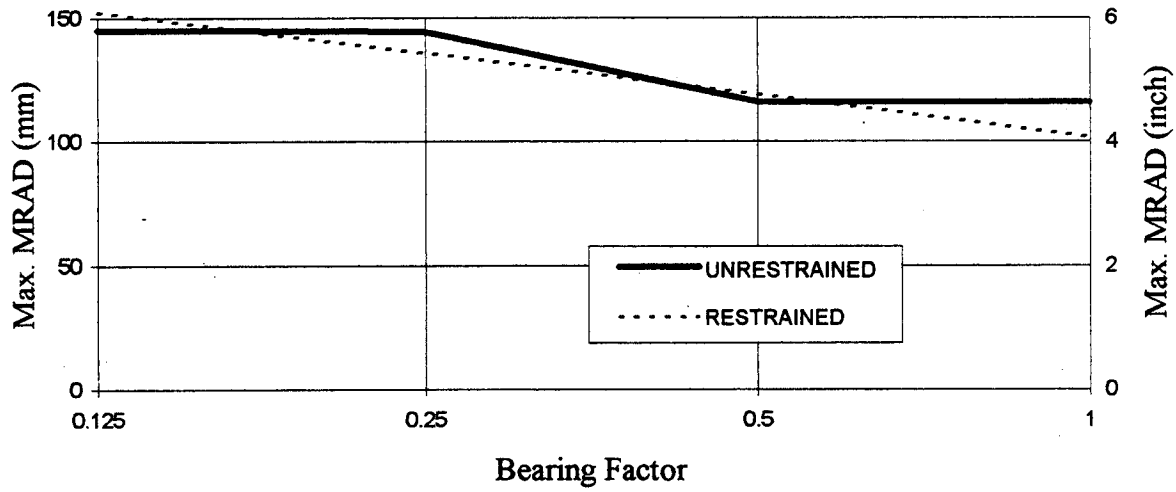

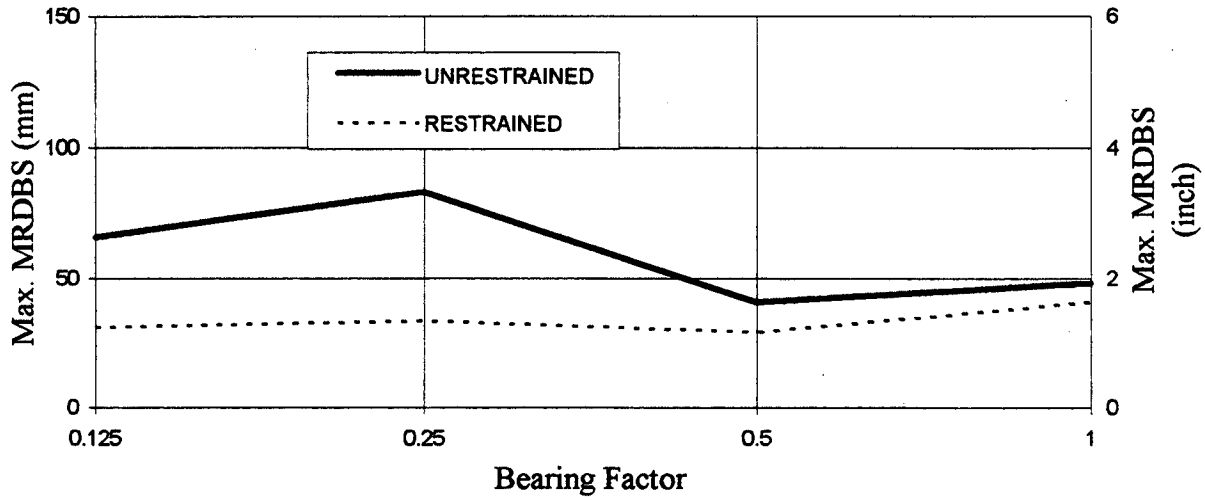

Figure 3.7. Effect of Restrainers on Configuration # 2

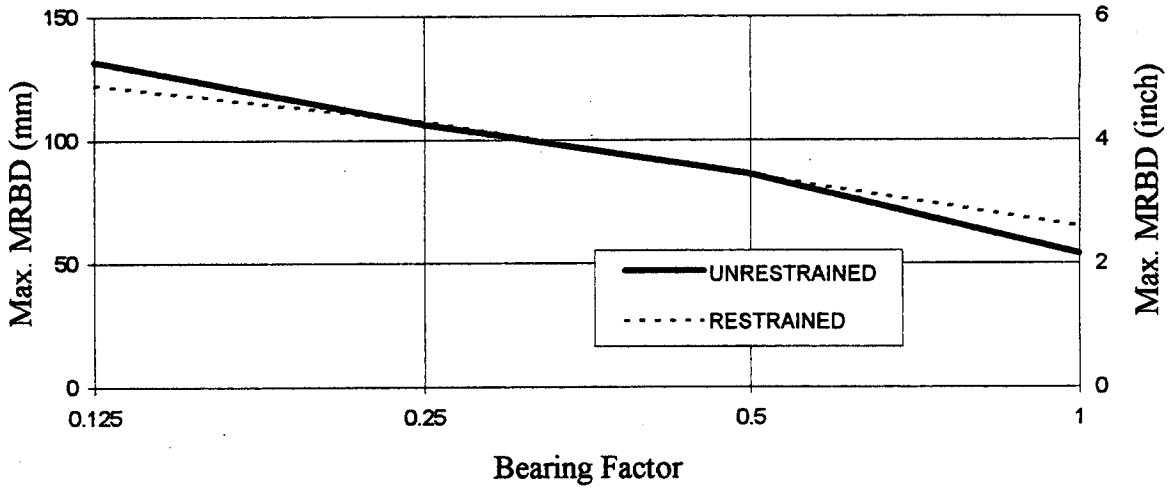

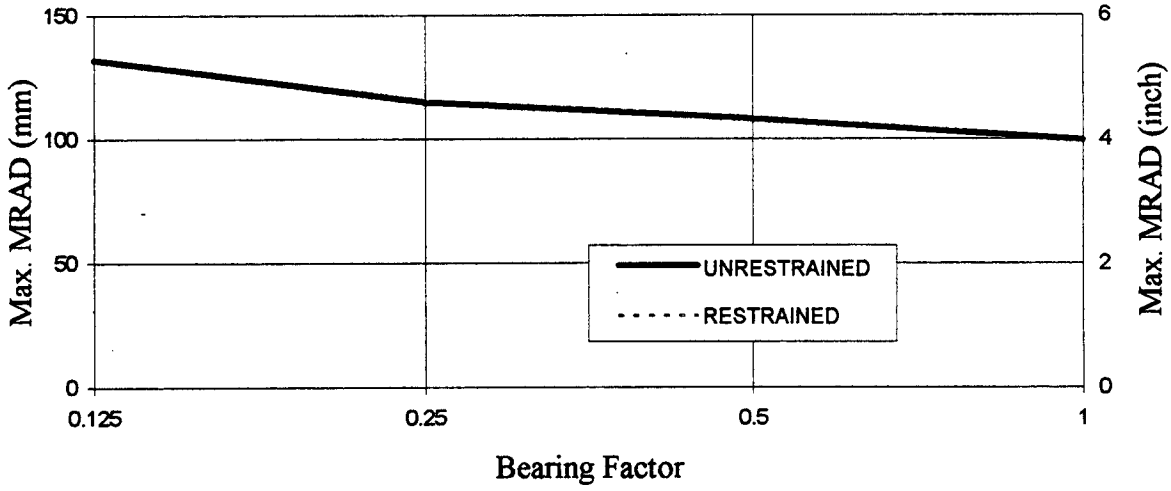

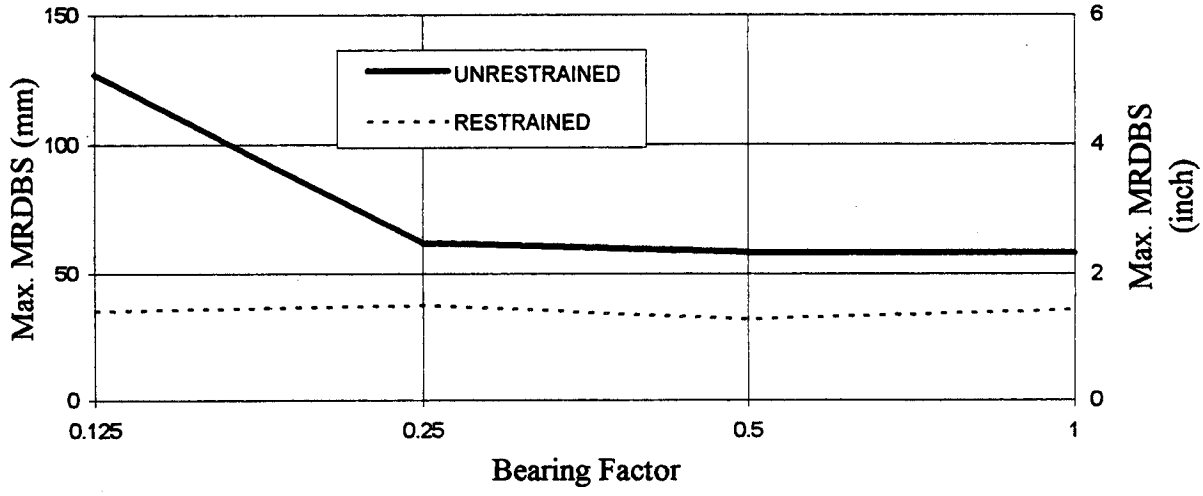

Figure 3.8. Effect of Restrainers on Configuration # 3

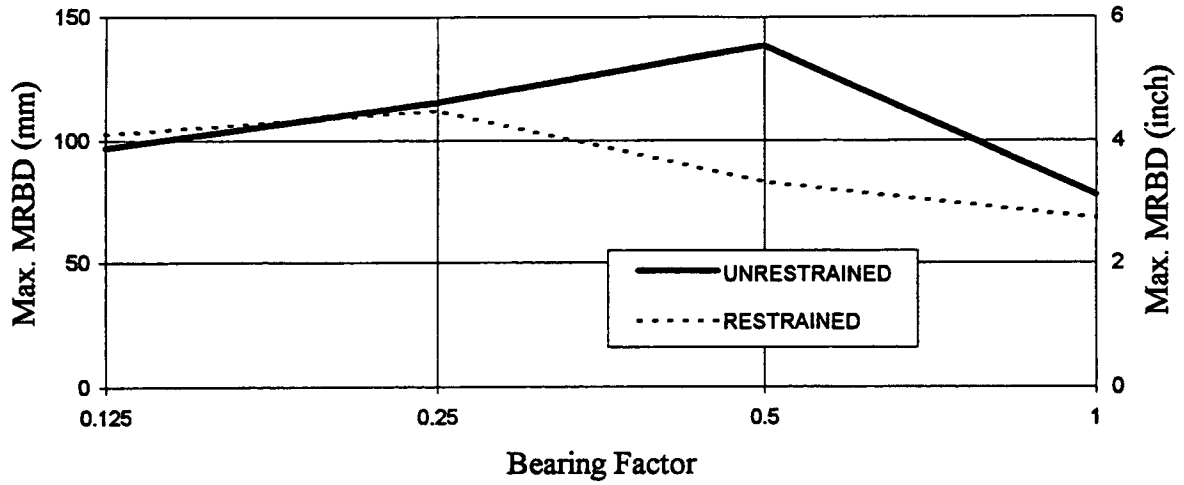

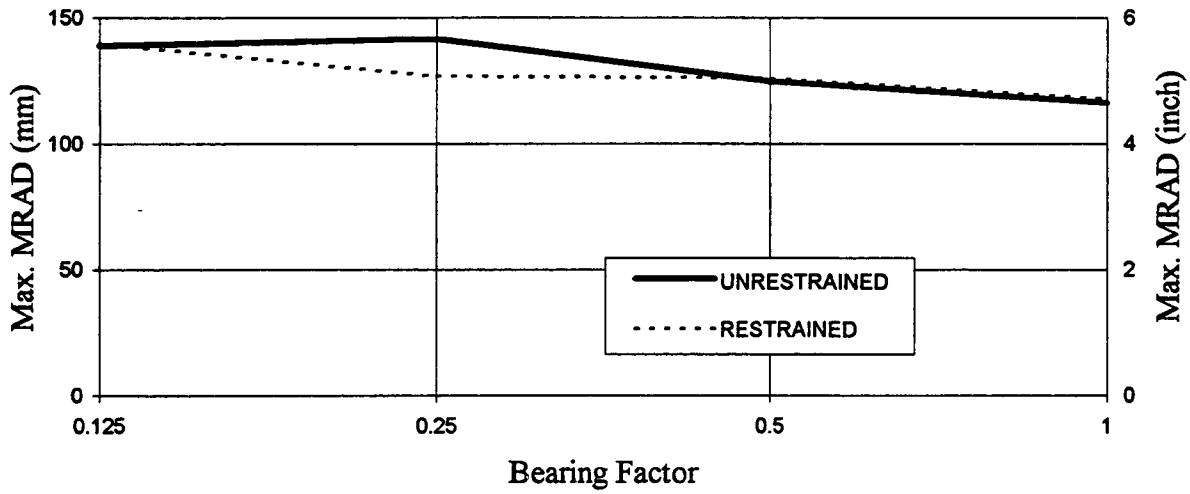

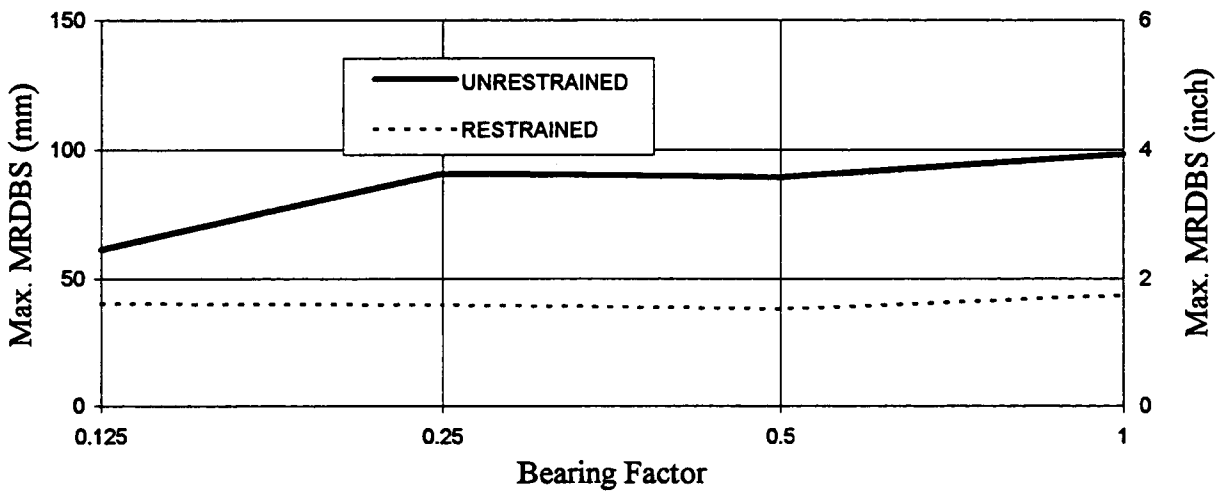

Figure 3.9. Effect of Restrainers on Configuration # 4

For the conditions studied here, the restrainers provided no benefit. In some cases, including the one that gave the largest MRAD (pier configuration #4 and bearing factor of 1/8), the presence of restrainers actually increased the MRAD. However, if a girder were to be unseated from its support, it might be able to hang from the restrainers, which would therefore provide a real benefit. However, if this were the designers' intention, the restrainers would have to be significantly stronger than is typically the case.

Cases in which the girder is tied directly to the pier cap were not investigated because WSDOT is not using that configuration.

CHAPTER 4

PROPOSED METHOD

The parametric study, reported in Chapter 3, identified the following three variables as important in predicting the MRBD:

- bearing pad friction
- earthquake record and intensity
- compression gap

The first two parameters listed above were also shown to be important predictors of the MRAD.

This chapter introduces a new method for identifying simply supported bridges that are prone to span unseating. The new procedure provides a means of predicting the MRBD and MRAD. These estimates can be compared with the available seat width to determine whether retrofit is necessary. Section 4.1 describes the proposed procedure, which relies on an equivalent stiffness and a response spectrum to estimate the MRBD and MRAD. Section 4.2 provides an example of the procedure applied to the standard model (Figure 2.1).

4.1 PROPOSED METHOD

While conducting the parametric study, the researchers found that the maximum MRBD generally occurred at the stiffest of the two outside piers. A plausible explanation for this observation is that the stiffer column induces larger forces in the bearing, which is

therefore more likely to suffer slip. Therefore, the proposed method focuses on estimating the MRBD at this location.

The proposed method idealizes all the components from the stiffest outside pier to the abutment at the opposite end as an equivalent single-degree-of-freedom (SDOF) system. The steps in this procedure are listed below.

Step 1 Construct the force-displacement relationship for the equivalent SDOF system. The bearings are modeled as elasto-plastic with a stiffness computed as shown below.

$$K_{bear} = \Sigma F_b / \Sigma C_g \quad (4.1)$$

where

ΣF_b = sum of the friction forces of all the pads between the stiffest outside pier and the abutment at the opposite end

ΣC_g = sum of all the compression gaps between the stiffest outside pier and the abutment at the opposite end

At a displacement of ΣC_g, the bearings yield (zero tangential stiffness) and the abutment is activated. The abutment is modeled as elasto-plastic.

Step 2 Guess a trial displacement (Δ_{trial}).

Step 3 Calculate the equivalent stiffness (K_{eq}) using the force-displacement relationship constructed in step 1 and the trial displacement.

Step 4 Calculate the equivalent period (T_{eq}) of the SDOF system.

$$T_{eq} = 2\pi\sqrt{W / (K_{eq} * g)} \quad (4.2)$$

where

W = weight of all mobilized spans

g = acceleration of gravity

Step 5 Calculate the equivalent spectral acceleration (ARS_{eq}).

$$ARS_{eq} = ARS * (A_{eq} / A_{sdof}) \quad (4.3)$$

where

ARS = spectral acceleration corresponding to the equivalent period

A_{eq} = area under equivalent force-displacement plot (to Δ_{trial})
= $1/2*K_{eq}*(\Delta_{trial})^2$

A_{sdof} = area under force-displacement plot constructed in step 1

The factor of A_{eq}/A_{sdof} is intended to account for variations in energy dissipation.

Step 6 Calculate the equivalent SDOF displacement (Δ_{sdof}).

$$\Delta_{sdof} = ARS_{eq} * (W / K_{eq}) \quad (4.4)$$

Step 7 Repeat steps 2 through 6 until the trial displacement equals the SDOF displacement.

Step 8 Calculate the predicted MRBD.

$$\text{Predicted MRBD} = 0.5 * \Delta_{sdof} \quad (4.5)$$

The form of Δ_{sdof} was selected because the MRBD must be related to the dynamic properties of the bridge elements. The value 0.5 in equation 4.5 was obtained by correlating values predicted using nonlinear time history analysis with the calculated Δ_{sdof}.

The same procedure can be used to predict the maximum MRAD. However, instead of constructing the force-displacement relationship from the stiffest outside pier to the abutment at the opposite end, the force-displacement relationship is constructed from one abutment to the other.

4.2 EXAMPLE

The standard bridge model described in Chapter 2 (Figure 2.1) and the idealized El Centro*2 acceleration response spectrum (Figure 4.1) were used to illustrate the procedure.

Step 1 Construct the force-displacement relationship.

$$K_{bear} = \mu (W_1 + W_2 + W_3) / 3 C_g = 0.3(3420 + 3420 + 2140)/3(25)$$

$$= 35.9 \text{ KN/mm } (205 \text{ kips/in.})$$

The system stiffness is equal to K_{bear} until the displacement equals $3C_g$. Thereafter, the bearing force is taken as the friction value.

At $\Delta = 3C_g$, the abutment becomes effective

At $\Delta = 3C_g + F_{abut}/K_{abut}$, the abutment yields

The force-displacement relationship is shown in Figure 4.2.

Step 2 Guess $\Delta_{trial} = 200$ mm (7.9 in.)

Step 3 Calculate the equivalent stiffness.

$$K_{eq} = (\mu (W_1 + W_2 + W_3) + F_{abut}) / \Delta_{trial}$$

$$= [0.3(3420 + 3420 + 2140) + 5080]/200$$
$$= 38.9 \text{ KN/mm } (222 \text{ kips/in.})$$

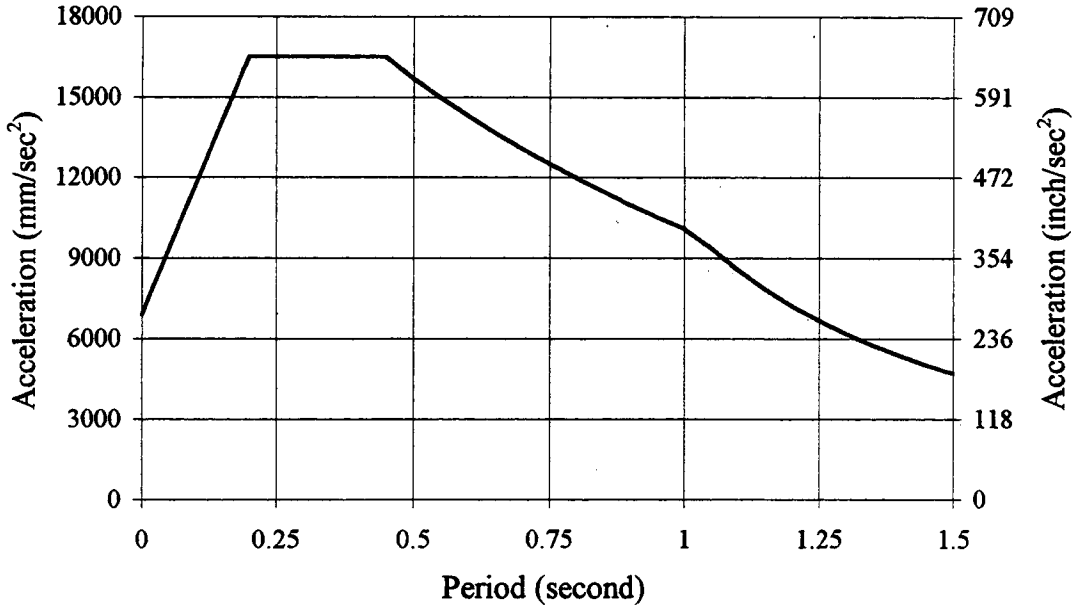

Figure 4.1. Idealized Acceleration Response Spectrum for El Centro*2

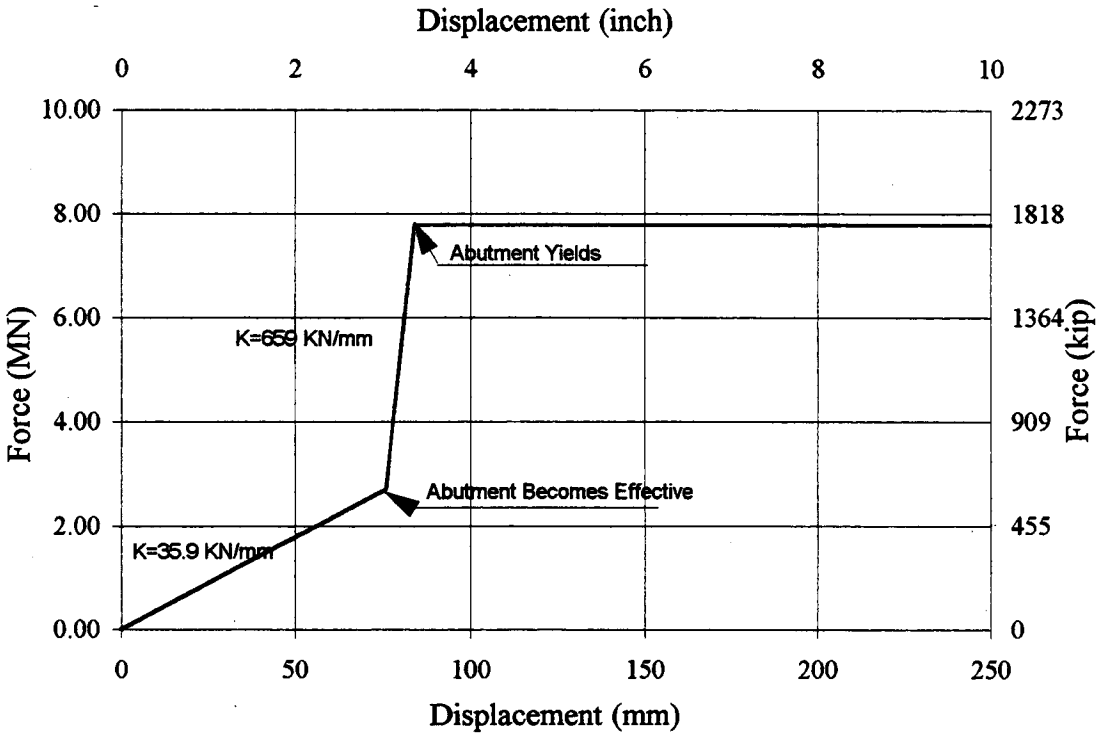

Figure 4.2. Force-Displacement Relationship for Example Bridge

Step 4 Calculate the equivalent period.

$$T_{eq} = 2\pi \sqrt{W / (K_{eq} * g)} = 2\pi \sqrt{8980 / (38.9 * 9810)} = 0.95 \text{ sec}$$

Step 5 Calculate the equivalent spectral acceleration.

From Figure 4.1, ARS = 10,500 mm/sec^2 (413 in./sec^2)

A_{eq} = 1/2 K_{eq} Δ_{trial}^2

= 1/2 * 38.9 * 200^2/1000

= 780 MN-mm (6930 kip-in.)

Figure 4.2 shows that

Abutment becomes effective at (76.2 mm, 2.74 MN)

Abutment yields at an additional force

= 5.08 MN (see Section 2.2)

and Δ = 5.08 MN/659 kN/MN = 7.7 MN

$\therefore$total Δ = 76.2 + 7.7 = 83.9 MN

total force= 2.74 + 5.08 MN = 7.82 MN

A_{sdof} = area under curve in Figure 4.2 up to Δ = 200 mm

= (1/2 * 76.2 MN * 2.74 MN)

+ ((2.74 + 7.82 MN)/2 * 7.7 mm)

= ((200 - 83.9 MN) * 7.82 MN)

A_{sdof} = 1100 MN-mm (9750 kip-in.)

ARS_{eq} = 10,500 (780/1100) = 7450 mm/sec^2 = 0.76 g

Step 6 Calculate the equivalent SDOF displacement.

$$\Delta_{sdof} = ARS_{eq} * W / K_{eq} = 0.76 (8980/38.9) = 175 \text{ mm } (6.9 \text{ in.})$$

Step 7 175 mm ≠ 200 mm, therefore repeat steps 2 through 6.

The process (steps 2 through 6) converged to Δ_{sdof} = 170 mm (6.7 in.)

Step 8 Compute the predicted MRBD.

Predicted MRBD = Δ_{sdof} / 2 = 170/2 = 85 mm (3.3 in.)

This predicted MRBD compares favorably with the nonlinear time history (NLTH) MRBD of 91 mm (3.6 in.).

4.3 COMPARISON OF PROPOSED METHOD WITH NLTH

The design procedure was repeated for 52 cases, including those considered in the parametric study (Chapter 3). Figure 4.3 shows how the predicted MRBD compared with the NLTH MRBD. The largest unconservative error was 38 mm (1.5 in.), and the average error was 18 mm (0.7 in.).

The same procedure was repeated to predict the MRAD. The only difference in procedure is that the equivalent SDOF system began at one abutment and ended at the other. This difference resulted in an additional span and compression gap being incorporated into the force-displacement relationship. A comparison between the estimates provided by the proposed method and the results of nonlinear analysis is shown in Figure 4.4. The average error was 23 mm (0.9 in.).

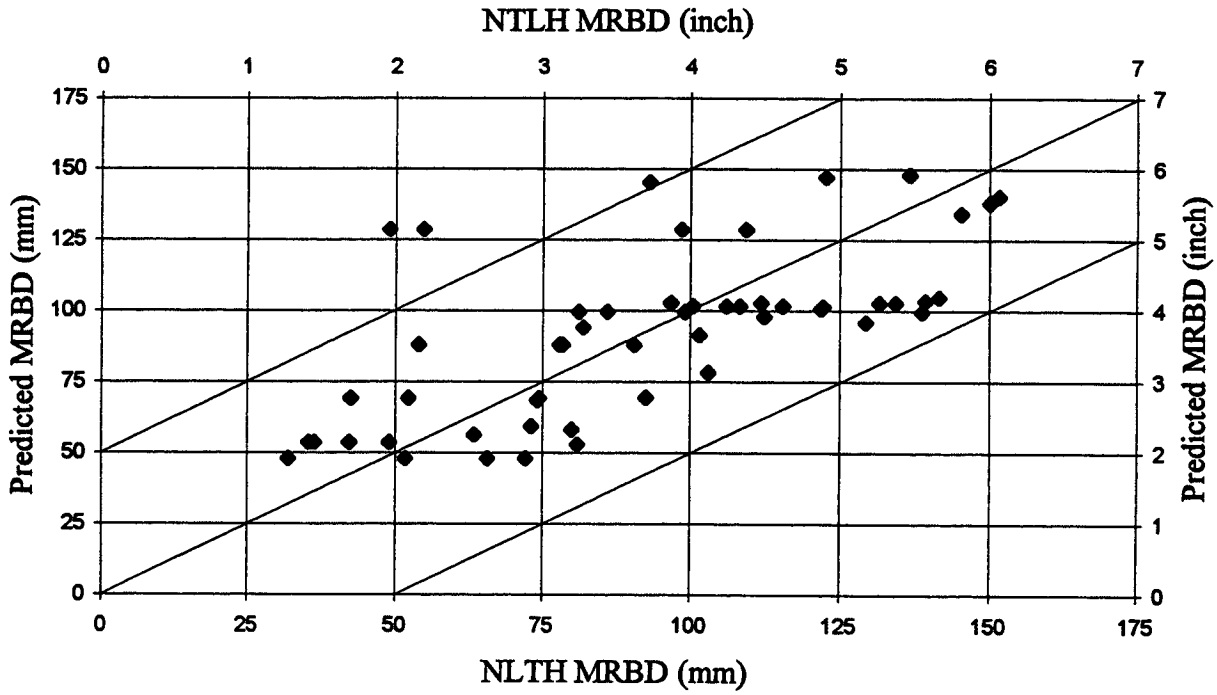

Figure 4.3. Comparison between Proposed Method MRBD and NLTH MRBD

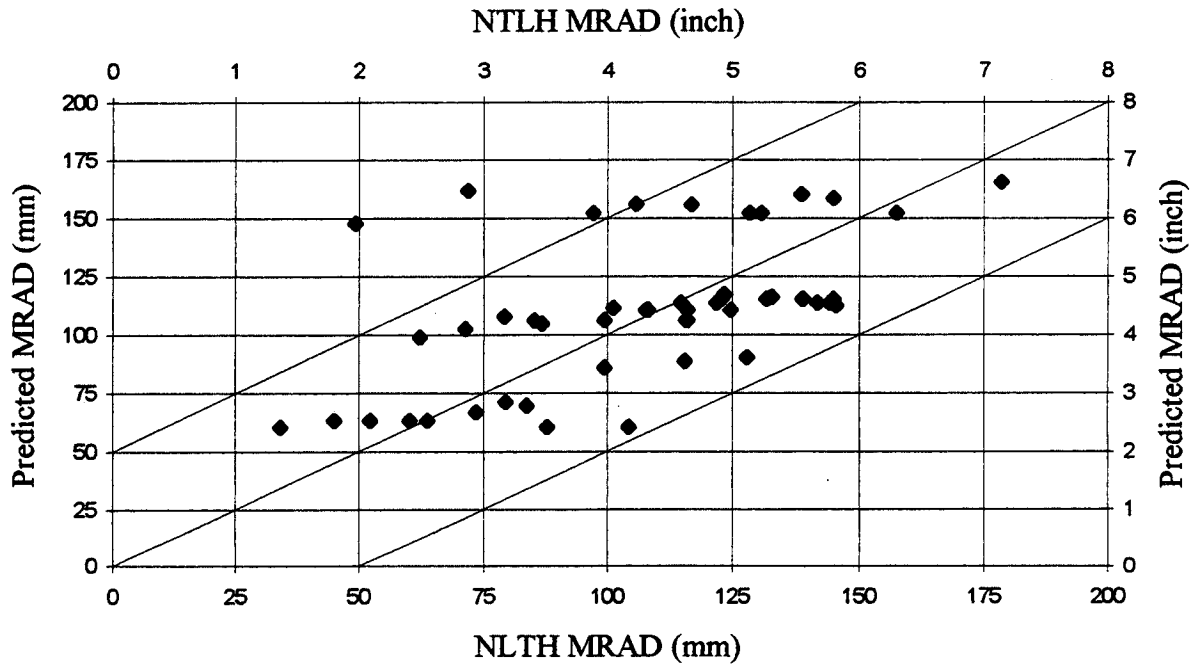

Figure 4.4. Comparison between Proposed Method MRAD and NLTH MRAD

4.4 DISCUSSION

If a pier is weak and its bearings are strong, the pier will move along with the second span, resulting in a smaller MRBD. In contrast, if the pier is strong and the bearings are weak, the pier will be able to oscillate almost independently of the second span, resulting in a larger MRBD. Note that the database used to develop the proposed method did not include any cases in which the stiffest outside pier had a height of more than 6.1 m (20 ft). Because the proposed method ignores pier height, it might not provide accurate results for bridges with tall outside piers.

CHAPTER 5

CONCLUSIONS AND RECOMMENDATIONS

A limited parametric study was conducted on simply supported bridges to determine the variables important in predicting span unseating. Sixty-eight nonlinear time history analyses were performed to determine the effect of varying six parameters. Restrainers were included in sixteen analyses. The remaining analyses did not include restrainers, and they were used to develop a new method for identifying unrestrained, simply supported bridges that are prone to span unseating. The effectiveness of restrainers connecting adjacent spans was also examined. The conclusions drawn from this work are discussed in this chapter.

5.1 CONCLUSIONS

1. The maximum relative bearing displacement (MRBD) depends most on the following three variables:
   - bearing pad friction resistance
   - earthquake record and intensity
   - compression gap
2. The following two variables significantly affect the maximum relative abutment displacement (MRAD):
   - bearing pad friction resistance
   - earthquake record and intensity
3. In all cases, the MRBD was less than 6 in., which is less than the typical allowable movement. However, further research is needed to estimate the effects of ground motion incoherency and to verify that the displacements are small for skewed bridges and bridges with larger compression gaps.

4. Sixteen of the analyses contained restrainers. In those analyses, the restrainers were found to be ineffective in reducing the MRBD. However, only a limited number of geometries was considered, and none of the analyses included girder compression stops. In bridges that contain compression stops, it is likely that the restrainers would be effective in reducing the MRBD.

5. A new method for predicting the maximum unrestrained MRBD and MRAD was introduced. This method provides results that match NLTH analysis to within 50 mm (2 in.).

6. In the complete set of 68 nonlinear analyses, the maximum MRBD never exceeded 155 mm (6.1 in.) and the maximum MRAD was approximately 180 mm (7.1 in.). For many bridges, these relative displacements would not be large enough to cause span unseating.

5.2 NEED FOR FURTHER RESEARCH

In this study, 68 nonlinear time history analyses were performed to consider the effect of varying six parameters. Additional parameters such as the number of spans and vertical accelerations need to be examined to ensure that the proposed method is acceptable.

The analyses showed that the friction resistance in the bearing pads greatly affects the MRBD and MRAD. The friction resistance of the bearing pads depends on the vertical load applied to the pads. Therefore, vertical accelerations could affect the relative displacements. Because the new method can account for variations in bearing friction resistance, it might be possible to incorporate the effects of vertical accelerations. Additional analyses that include vertical acceleration effects should be conducted to determine the effect of vertical motion.

The proposed method was shown to provide accurate results for the maximum MRBD and MRAD. However, the researchers did not examine the accuracy of this

method at other bearing locations. The new method should be tested to investigate whether it provides accurate results at other bearing locations.

The effectiveness of restrainers connecting the pier cap to the adjacent span was not studied. Research needs to be conducted to determine whether this method is an effective way of reducing the MRBD. Research also needs to be conducted to incorporate the effect of skew.

REFERENCES

American Association of State Highway and Transportation Officials (1992). *Standard Specifications for Highway Bridges*, 15th ed. Washington, D.C.

California Department of Transportation (1989, October). *Bridge Design Aids.* Sacramento, California.

Lwin, M. M., and Henley, E. H. (1993, September). "Bridge Seismic Retrofit Program Report." Washington State Department of Transportation, Olympia, Washington.

Trochalakis, P., Eberhard, M.O., and Stanton, J. F. (1996, May). "Design of Seismic Restrainers for In-Span Hinges" (WA-RD 387.2), Technical Report, Washington State Department of Transportation, Olympia, Washington.

NOTATION

MRAD = Maximum relative abutment displacement

MRBD = Maximum relative bearing displacement

MRDBS = Maximum relative displacement between adjacent spans

NLTH = Nonlinear time history

SDOF = Single degree of freedom

APPENDIX A
DATABASE

DATABASE FOR UNRESTRAINED BRIDGES WITH SIMPLY SUPPORTED SPANS

DIRECTORY/FILE	REL. DISP. @ 2	REL. DISP. @ 3	REL. DISP. @ 4	ABUT. 1 TO BEAM	ABUT. 2 TO BEAM	MRAD 1	MRHD 2L	MRHD 2R	MRHD 3L	MRHD 3R	MRHD 4L	MRHD 4R	MRAD 5
SIMPLY/STANDK0	1.46	0.05	1.90	4.92	5.27	4.00	0.30	3.09	0.22	0.30	1.06	1.20	4.56
SIMPLY/K2K1/05-1-05Z	3.68	0.20	3.43	2.41	3.62	2.41	1.02	3.57	0.40	0.25	2.67	1.59	3.36
SIMPLY/K2K1/075-1Z	2.28	0.82	0.79	3.48	4.54	3.48	0.80	2.13	1.02	0.24	1.55	0.61	3.92
SIMPLY/K2K1/15-1-05Z	1.60	1.50	3.87	5.40	1.38	4.57	1.47	0.52	2.03	0.33	3.07	1.93	1.16
SIMPLY/ABUT/AB025F1	1.68	0.75	1.61	7.04	5.79	4.86	3.85	5.57	4.10	4.47	5.39	3.65	4.47
SIMPLY/ABUT/AB025F02	3.52	0.38	2.98	5.03	3.44	3.99	2.32	4.80	2.69	3.25	4.14	3.42	3.34
SIMPLY/ABUT/AB025F05	2.89	0.27	2.98	3.72	1.98	3.42	1.45	5.09	0.89	0.08	2.93	3.02	1.98
SIMPLY/ABUT/AB025F1	2.81	0.70	2.59	2.93	2.21	2.45	1.22	4.00	0.53	0.37	2.97	2.03	1.17
SIMPLY/ABUT/AB05F012	2.26	1.20	3.60	6.43	5.12	5.23	2.57	5.48	3.21	4.63	4.27	4.22	4.27
SIMPLY/ABUT/AB05F025	2.76	0.25	3.43	6.53	4.05	5.73	2.05	4.81	2.80	2.09	3.63	3.47	3.34
SIMPLY/ABUT/AB05F05	2.23	0.56	3.77	3.70	2.01	3.12	1.52	4.43	0.59	0.83	3.62	2.25	1.98
SIMPLY/ABUT/AB05F1	2.93	0.41	3.89	2.81	2.83	2.81	1.48	3.23	0.43	0.14	2.71	1.76	2.30
SIMPLY\BEARING\EIGHTH\05-1-05Z	2.46	4.03	1.42	6.23	5.60	4.84	2.87	4.10	2.23	4.20	4.41	2.63	4.63
SIMPLY\BEARING\EIGHTH\075-1Z	5.00	1.32	1.86	5.71	5.50	5.19	1.49	5.18	2.82	2.94	3.36	2.79	4.23
SIMPLY\BEARING\EIGHTH\15-1-05Z	2.09	2.41	2.27	5.88	5.67	5.47	1.93	2.43	2.53	3.81	3.46	2.86	4.09
SIMPLY\BEARING\EIGHTH\STANDARD	2.59	2.50	1.68	6.51	6.03	5.71	1.33	5.29	3.11	3.32	4.19	2.62	4.37
SIMPLY\BEARING\HALF\K0\05-1-05Z	2.19	1.27	3.33	4.08	4.67	2.97	2.43	3.11	1.59	0.20	3.90	1.84	4.26
SIMPLY\BEARING\HALF\K0\075-1Z	2.29	0.88	2.18	4.79	4.43	4.25	0.74	3.39	0.35	1.69	2.50	1.92	3.70
SIMPLY\BEARING\HALF\K0\15-1-05Z	1.91	2.67	3.52	5.89	2.65	4.91	2.44	0.61	5.46	0.15	3.36	2.33	2.03
SIMPLY\BEARING\HALF\K0\STANDARD	1.30	0.13	1.61	5.49	5.08	4.57	0.97	2.36	0.48	0.23	3.20	0.43	4.10
SIMPLY\BEARING\QUARTER\K0\05-1-05Z	2.21	1.87	1.97	5.58	4.87	4.80	2.18	3.96	1.88	2.53	3.78	2.27	4.20
SIMPLY\BEARING\QUARTER\K0\075-1Z	2.44	0.80	2.22	5.32	4.98	4.43	1.26	4.18	1.81	2.09	3.70	1.71	4.52
SIMPLY\BEARING\QUARTER\K0\15-1-05Z	1.35	2.92	3.57	7.11	4.06	5.58	3.00	1.05	3.18	2.31	4.55	2.69	3.42
SIMPLY\BEARING\QUARTER\K0\STANDARD	3.27	0.81	1.48	6.39	6.02	5.68	1.24	4.27	3.50	1.39	3.86	1.36	4.52
SIMPLY\COMPGAP\K2K1\05-1-05Z	3.66	0.18	3.34	1.94	1.11	1.94	1.80	4.31	0.28	0.44	2.25	1.86	1.11
SIMPLY\COMPGAP\K2K1\05-1EIGH	2.67	1.57	1.13	7.03	5.90	7.03	2.25	5.97	4.57	3.27	5.58	2.27	5.90
SIMPLY\COMPGAP\K2K1\05-1HALF	3.45	0.00	1.48	4.17	2.31	4.17	1.96	5.72	0.30	1.54	2.87	2.23	2.31
SIMPLY\COMPGAP\K2K1\05-1QUAR	5.58	0.00	4.98	2.87	2.33	2.83	2.13	5.91	3.49	2.14	4.35	2.14	2.33
SIMPLY\COMPGAP\K2K1\075-1Z	3.69	1.63	0.59	3.32	2.95	3.32	0.38	3.88	1.80	0.36	0.75	0.31	2.92
SIMPLY\COMPGAP\K2K1\15-1-05Z	1.73	1.63	3.36	5.92	1.16	5.92	1.05	0.73	1.65	0.38	2.16	1.88	1.16
SIMPLY\COMPGAP\K2K1\STANDK0	1.92	0.00	1.08	4.08	4.36	4.08	0.75	1.93	0.25	0.32	1.44	0.27	4.29

DIRECTORY/FILE	REL. DISP. @ 2	REL. DISP. @ 3	REL. DISP. @ 4	ABUT. 1 TO BEAM	ABUT. 2 TO BEAM	MRAD 1	MRHD 2L	MRHD 2R	MRHD 3L	MRHD 3R	MRHD 4L	MRHD 4R	MRAD 5
SIMPLY\JAMES1\05-1-05Z	1.77	0.13	2.52	1.35	0.62	1.35	0.96	2.56	0.22	0.17	2.59	0.95	0.62
SIMPLY\JAMES1\05-1EIGH	0.77	0.00	1.24	4.44	5.47	4.44	2.16	3.43	2.73	2.27	4.06	1.65	5.04
SIMPLY\JAMES1\05-1HALF	0.78	0.00	1.55	3.92	2.88	3.92	1.36	2.83	0.09	0.48	3.19	1.19	2.85
SIMPLY\JAMES1\05-1QUAR	0.84	0.08	0.74	4.26	4.78	4.26	1.72	3.19	1.69	1.74	3.65	1.49	4.55
SIMPLY\JAMES1\075-1Z	1.84	0.19	0.57	2.00	3.47	2.00	0.31	2.04	0.21	0.29	0.54	0.40	3.46
SIMPLY\JAMES1\15-1-05Z	1.60	0.35	2.65	3.51	0.74	3.51	1.15	0.62	0.25	0.37	2.84	0.98	0.68
SIMPLY\JAMES1\STANDK0	1.10	0.00	1.00	3.26	4.20	3.26	0.35	1.26	0.19	0.18	0.47	0.64	4.11
SIMPLY\PACOIMA\05-1-05Z	1.74	0.64	2.30	3.96	3.17	3.83	1.41	2.92	0.41	0.29	2.51	1.41	3.17
SIMPLY\PACOIMA\05-1EIGH	4.26	1.41	1.45	6.77	7.60	5.46	3.26	5.38	5.13	2.85	4.63	4.08	5.37
SIMPLY\PACOIMA\05-1HALF	1.86	1.53	2.02	5.34	5.37	4.60	1.89	3.54	0.99	0.94	3.67	2.56	4.15
SIMPLY\PACOIMA\05-1QUAR	1.28	1.55	2.83	6.62	6.68	5.71	2.20	4.83	3.40	1.52	3.99	3.37	4.87
SIMPLY\PACOIMA\075-1Z	2.05	0.11	0.60	5.32	4.22	5.15	0.41	2.08	0.33	0.10	0.80	0.23	4.22
SIMPLY\PACOIMA\15-1-05Z	1.10	1.93	3.52	5.82	3.14	5.06	0.72	0.50	1.83	0.26	2.93	1.81	2.87
SIMPLY\PACOIMA\STANDK0	1.26	0.33	1.12	6.94	5.66	6.20	0.47	1.59	0.43	0.24	1.68	0.25	4.77
SIMPLY\OLYMPIA\05-1-05Z	1.72	0.35	2.01	2.37	0.55	2.37	0.76	1.93	0.25	0.28	1.71	1.14	0.55
SIMPLY\OLYMPIA\05-1EIGH	0.71	0.00	1.36	3.13	2.65	3.13	1.02	2.88	1.22	1.84	2.51	1.09	2.65
SIMPLY\OLYMPIA\05-1HALF	1.79	0.00	2.33	2.90	0.45	2.90	0.30	2.50	0.10	0.80	1.62	1.40	0.45
SIMPLY\OLYMPIA\05-1QUAR	1.75	0.84	1.83	3.30	1.10	3.30	1.08	3.15	0.12	1.70	1.72	1.21	1.10
SIMPLY\OLYMPIA\075-1Z	1.44	0.67	0.82	1.78	1.50	1.78	0.52	1.44	0.41	0.35	0.78	0.77	1.50
SIMPLY\OLYMPIA\15-1-05Z	1.48	1.06	2.06	2.51	0.42	2.51	1.16	0.59	0.39	0.82	1.67	1.10	0.42
SIMPLY\OLYMPIA\STANDK0	1.57	0.38	1.83	2.06	1.13	2.06	0.30	1.40	0.15	0.39	1.34	0.82	1.13

DATABASE FOR RESTRAINED BRIDGES WITH SIMPLY SUPPORTED SPANS (ALL CASES Kr=500)

DIRECTORY/FILE	REL. DISP. @ 2	REL. DISP. @ 3	REL. DISP. @ 4	ABUT. 1 TO BEAM	ABUT. 2 TO BEAM	MRAD 1	MRHD 2L	MRHD 2R	MRHD 3L	MRHD 3R	MRHD 4L	MRHD 4R	MRAD 5
EIGHTH/K500/05-1-05Z	1.32	1.26	1.31	5.75	5.74	4.74	2.39	4.19	2.50	3.92	4.30	2.27	4.85
EIGHTH/K500/075-1Z	1.29	1.37	1.31	5.94	5.95	5.18	1.63	4.81	2.96	3.02	4.02	2.34	4.49
EIGHTH/K500/15-1-05Z	1.36	1.59	1.38	6.43	6.02	5.51	1.88	2.69	2.87	3.18	4.04	2.81	4.68
EIGHTH/K500/STANDARD	0.91	0.79	1.24	6.79	6.46	6.00	1.17	5.03	3.06	3.37	4.07	2.62	4.57
HALF/K500/05-1-05Z	1.36	0.77	1.39	4.41	3.63	3.81	1.88	3.35	0.69	0.49	3.44	1.69	3.21
HALF/K500/075-1Z	1.24	1.05	1.18	4.42	4.43	4.25	0.62	3.38	0.35	1.55	2.50	1.70	3.70
HALF/K500/15-1-05Z	1.09	1.51	1.47	5.92	3.64	4.96	0.78	1.50	3.00	0.03	3.27	2.28	2.72
HALF/K500/STANDARD	1.17	0.34	1.10	5.49	5.67	4.57	0.95	2.05	0.34	0.84	2.96	0.10	4.69
QUARTER/K500/05-1-05Z	1.23	1.34	1.28	5.45	5.18	4.85	2.09	3.90	2.47	2.37	3.78	2.49	4.21
QUARTER/K500/075-1Z	1.33	1.28	1.45	5.07	4.91	4.12	1.28	3.93	2.19	2.10	4.23	1.71	4.50
QUARTER/K500/15-1-05Z	1.43	1.55	1.57	6.60	5.91	4.99	2.88	0.31	2.02	3.63	4.41	2.46	4.82
QUARTER/K500/STANDARD	1.33	1.31	1.20	6.08	6.26	5.34	1.00	4.30	3.23	2.08	4.62	0.83	4.79
K2K1/K500/05-1-05Z	1.59	0.58	1.50	3.50	3.65	2.52	1.31	3.06	0.42	0.70	2.29	1.85	3.21
K2K1/K500/075-1Z	1.39	0.82	1.12	4.43	4.54	3.48	0.71	2.56	1.02	0.24	0.82	0.75	3.92
K2K1/K500/15-1-05Z	0.97	1.44	1.71	5.59	3.25	4.63	0.61	0.60	1.57	0.35	2.69	1.48	2.40
K2K1/K500/STANDARD	1.06	0.44	1.32	4.29	4.65	3.64	0.31	2.89	0.46	0.58	1.44	0.55	4.00